AEDC-TR-66-190

H Ball MAR 20 1967

INVESTIGATION OF THE EFFECT OF FLARE AND RAMP ANGLE ON THE UPSTREAM INFLUENCE OF LAMINAR AND TRANSITIONAL REATTACHING FLOWS FROM MACH 3 TO 7

J. Don Gray

ARO, Inc.

January 1967

Distribution of this document is unlimited.

VON KÁRMÁN GAS DYNAMICS FACILITY

ARNOLD ENGINEERING DEVELOPMENT CENTER

AIR FORCE SYSTEMS COMMAND

ARNOLD AIR FORCE STATION, TENNESSEE

NOTICES

When U. S. Government drawings specifications, or other data are used for any purpose other than a definitely related Government procurement operation, the Government thereby incurs no responsibility nor any obligation whatsoever, and the fact that the Government may have formulated, furnished, or in any way supplied the said drawings, specifications, or other data, is not to be regarded by implication or otherwise, or in any manner licensing the holder or any other person or corporation, or conveying any rights or permission to manufacture, use, or sell any patented invention that may in any way be related thereto.

Qualified users may obtain copies of this report from the Defense Documentation Center.

References to named commercial products in this report are not to be considered in any sense as an endorsement of the product by the United States Air Force or the Government.

INVESTIGATION OF THE EFFECT OF FLARE AND RAMP ANGLE ON THE UPSTREAM INFLUENCE OF LAMINAR AND TRANSITIONAL REATTACHING FLOWS AT MACH 3 TO 7

J. Don Gray
ARO, Inc.

Distribution of this document is unlimited.

AF AEDC
Arnold AFS Tenn

FOREWORD

This work was done at the request of the Air Force Flight Dynamics Laboratory (AFFDL), Flight Control Division, Air Force Systems Command (AFSC), under Program Element 62405364, Task 821902.

The results of this research were obtained by ARO, Inc. (a subsidiary of Sverdrup & Parcel and Associates, Inc.), contract operator of the Arnold Engineering Development Center (AEDC), AFSC, Arnold Air Force Station, Tennessee, under Contract AF40(600)-1200. The work was accomplished under ARO Project No. VT0530, and the manuscript was submitted for publication on September 7, 1966.

The author wishes to acknowledge the use of data supplied by H. R. Little and W. T. Strike of ARO, Inc.

This technical report has been reviewed and is approved.

James N. McCready
Major, USAF
AF Representative, VKF
Directorate of Test

Leonard T. Glaser
Colonel, USAF
Director of Test

ABSTRACT

An experimental investigation of laminar- and transitional-flow separation induced by flares and ramps of different angles was conducted at Mach numbers 3, 5, and 7 over a broad Reynolds number range. Surface pressure distributions, schlieren and shadowgraph pictures, and the oil film technique were used to determine the effect of transition during flow reattachment on the scale of laminar separation. It is concluded that because transition was always triggered prematurely by the reattachment pressure gradient, small flow deflections ($\theta \leq 10$ deg) are required when investigating laminar reattaching flows at similar test conditions. The scale of separation increased with Reynolds number increase, and the pressure distribution upstream of the flare was characterized by the absence of any lengthy plateau whenever the flow was laminar through the reattachment zone. Nose blunting reduced the extent of such separations.

CONTENTS

		Page
	ABSTRACT	iii
	NOMENCLATURE	viii
I.	INTRODUCTION	1
II.	APPARATUS	
	2.1 Wind Tunnels	2
	2.2 Models	2
	2.3 Instrumentation	3
	2.4 Oil Flow Technique	3
III.	RESULTS AND DISCUSSION	
	3.1 Pressure Distributions - Axisymmetric Model	4
	3.2 Pressure Distributions - Ramp Models	5
	3.3 Upstream Influence - Axisymmetric Models	6
	3.4 Transition Influence - Axisymmetric Models	7
	3.5 Transition Influence - Ramp Models	10
	3.6 Oil Film Data - Axisymmetric Models	10
	3.7 Separation Pressure Gradient	12
	3.8 Scaling of Separation Extent	13
IV.	CONCLUDING REMARKS	16
	REFERENCES	17

ILLUSTRATIONS

Figure		
1.	Test Facilities	19
2.	Model Configurations	20
3.	Effect of End Plates on Flow at $M_\infty = 3$, $\theta = 0$, $Re_c = 0.19 \times 10^6$	
	a. Without End Plates	21
	b. With End Plates	21
4.	Pressure Distributions for Sharp Cone Model, $\theta = 7.5$ deg, $\Delta x_c = 3.8$ in.	
	a. $M_\infty = 3$ and 7	22
	b. $M_\infty = 5$	23
5.	Pressure Distributions for Sharp Cone Model, $\theta = 10$ deg, $\Delta x_c = 3.8$ in.	
	a. $M_\infty = 3$	24
	b. $M_\infty = 5$	25
	c. $M_\infty = 7$	26

Figure		Page
6.	Pressure Distributions for Sharp Cone Model, θ = 15 deg	
	a. $M_\infty = 5$, $\Delta x_c = 2.6$ and 3.8 in.	27
	b. $M_\infty = 7$, $\Delta x_c = 3.8$ in.	28
7.	Effect of Flare Angle on Pressure Distribution for Sharp Cone Model	
	a. $M_\infty = 3$, $Re_c = 0.36 \times 10^6$	29
	b. $M_\infty = 7$, $Re_c = 1.47 \times 10^6$	29
8.	Pressure Distribution for Hemisphere Model, θ = 7.5 deg, $\Delta x_c = 3.8$ in.	
	a. $M_\infty = 3$ and 5	30
	b. $M_\infty = 5$ and 7	31
9.	Pressure Distribution for Hemisphere Model, θ = 10 deg, $\Delta x_c = 3.8$ in.	
	a. $M_\infty = 3$	32
	b. $M_\infty = 5$	33
	c. $M_\infty = 7$	34
10.	Pressure Distribution for Hemisphere Model, θ = 15 deg, $\Delta x_c = 3.8$ in. at $M_\infty = 5$ and 7	35
11.	Effect of Flare Angle on Pressure Distribution for Hemisphere Model, $\Delta x_c = 3.8$ in.	
	a. $M_\infty = 5$, $1.15 \leq (Re_c \times 10^{-6}) \leq 1.61$	36
	b. $M_\infty = 7$, $Re_c = 1.01 \times 10^6$	36
12.	Pressure Distribution for Flat Plate Model, $M_\infty = 3$, $x_c = 3.8$ in.	
	a. θ = 7.5 deg	37
	b. θ = 10 deg	38
	c. θ = 15 deg	39
13.	Effect of Ramp Angle on Pressure Distribution for Flat Plate Model, $M_\infty = 3$, $x_c = 3.8$, $Re_c = 0.205 \times 10^6$	40
14.	Upstream Influence versus Reynolds Number for Sharp Cone Model, $\Delta x_c = 3.8$ in.	
	a. $M_\infty = 3$	41
	b. $M_\infty = 5$, Tunnel D	41
	c. $M_\infty = 5$, Tunnel E	42
	d. $M_\infty = 7$	42

Figure		Page
15.	Upstream Influence versus Reynolds Number for Hemisphere Model, Δx_c = 3.8 in.	
	a. $M_\infty = 3$	43
	b. $M_\infty = 5$	43
	c. $M_\infty = 7$	43
16.	Relative Transition Location versus Reynolds Number for Sharp Cone Model, Δx_c = 3.8 in.	
	a. $M_\infty = 3$	44
	b. $M_\infty = 5$, Tunnel D	44
	c. $M_\infty = 5$, Tunnel E	45
	d. $M_\infty = 7$	45
17.	Schlieren Pictures of Sharp Cone Models, Δx_c = 3.8 in.	
	a. θ = Variable, $M_\infty = 3$, $Re_c = 0.90 \times 10^6$	46
	b. θ = 10 deg, $M_\infty = 3$, Re_c = Variable	47
	c. θ = 10 deg, $M_\infty = 5$, Re_c = Variable	48
18.	Shadowgraph Pictures of Sharp Cone Model, Δx_c = 3.8 in., θ = 7.5 deg, $M_\infty = 5$, Re_c = Variable	49
19.	Correlation of Reattachment Transition Increment with Upstream Influence for Sharp Cone Models	
	a. θ = 7.5 deg	50
	b. θ = 10 deg	51
	c. θ = 15 deg	52
20.	Relative Transition Location versus Reynolds Number for Flat Plate Model, x_c = 3.8 in., $M_\infty = 3$	53
21.	Correlation of Reattachment Transition Increment with Upstream Influence for Flat Plate Model, x_c = 3.8 in., $M_\infty = 3$	54
22.	Typical Oil Film Data for Sharp Cone Model, Δx_c = 3.8 in., $M_\infty = 3$, $Re_c = 0.36 \times 10^6$	
	a. θ = 5 deg	55
	b. θ = 7.5 deg	55
	c. θ = 10 deg	55
	d. θ = 20 deg	55
23.	Enlargement of Oil Film Picture for Sharp Cone Model, Δx_c = 3.8 in., $M_\infty = 3$, $Re_c = 0.90 \times 10^6$, θ = 10 deg.	56

Figure		Page
24.	Variation of Separation and Reattachment Locations with Reynolds Number at $M_\infty = 3$ on Sharp Cone Model, $\Delta x_c = 3.8$ in. . . .	57
25.	Separation Pressure Gradient versus Mach Number, Adiabatic Wall Data	58
26.	Separation Pressure Gradient versus Mach Number, Cold Wall Data.	59

NOMENCLATURE

c_f	Local laminar skin-friction coefficient, τ_w/q_∞
C_p	Pressure coefficient, $(p - p_\infty)/q_\infty$
M	Mach number
p	Surface pressure, psia
q	Dynamic pressure, psia
Re	Reynolds number based on free-stream conditions and length x
T	Temperature, ^oR
T_o	Stilling chamber temperature, ^oR
x	Wetted length from nose, in.
Δx_c	Cylinder length to flare, in.
y	Normal distance, in.
γ	Ratio of specific heats
δ	Laminar boundary-layer total thickness, in.
θ	Flare or ramp angle, deg
τ_w	Shear stress at wall, psi

SUBSCRIPTS

c	Ramp leading edge
m	Midpoint of pressure rise
o	Beginning of interaction
r	Reattachment
s	Separation
t	Beginning of transition
w	Wall
∞	Free stream

SECTION I
INTRODUCTION

An experimental study was made to determine how large the flare angle may be before transition moves into the reattachment zone. This study was made as a part of a general program, supported by the Air Force Flight Dynamics Laboratory, to provide ultimately experimental data showing the effects of wall cooling on the surface pressure distribution for laminar, supersonic, and hypersonic flows. These data, which are required to verify the theoretical method of Nielsen, Lynes, and Goodwin (Ref. 1), were originally expected to be obtained with the same configuration as used in the investigation by Abbott, Holt, and Nielsen (Ref. 2).

However, after conducting the first experiments (in 1965) at Mach number 3 and 5 with the original 30-deg semi-angle flare configuration without cooling, it became increasingly evident that such large flares probably triggered transition during flow reattachment. Although the experiments of Gray (Ref. 3) for laminar boundary-layer separation seemed to show that the proximity of transition to reattachment did not necessarily change the influence of Reynolds number on the extent of separation, considerable doubt on Gray's classification of the type of flow separation was raised by the results of Ginoux (Refs. 4 and 5) which were in substantial agreement with the work of Gadd, Holder, and Regan (Ref. 6). These works indicated that a negligible plateau was characteristic of laminar reattaching flows despite the implications to the contrary in the work of Chapman, Kuehn, and Larson (Ref. 7).

Surface pressure measurements were first made on the centerbody only of the conical nose model to measure the variation of upstream influence with Reynolds number as affected by small flare angle changes at Mach 3. Schlieren pictures, obtained at the same time, indicated the effect of transition was like that shown by Ref. 6. Therefore, instrumented flares were built to obtain data on the recompression process, and tests were then conducted with three flares (7.5-, 10-, and 15-deg semi-angle) at Mach 3, 5, and 7 with both a sharp cone and hemispherical nose cylinder over the maximum range of Reynolds Number. Surface pressure measurements at only Mach 3 were obtained with a flat plate model with a trailing edge ramp, for ramp angles of 7.5, 10, and 15 deg over the maximum Reynolds number range.

SECTION II
APPARATUS

2.1 WIND TUNNELS

The tests were made in the 12-in. supersonic and hypersonic tunnels (Gas Dynamic Wind Tunnels, Supersonic D and Hypersonic E) (Fig. 1), both of which are intermittent, variable density wind tunnels with 12- by 12-in.^{2} test sections. Tunnel D was operated at Mach numbers of 3 and 5 at stagnation pressures from about 2 to 60 psia and at temperatures of about 520°R. Tunnel E was operated at Mach numbers of 5 and 7 at stagnation pressures from about 100 to 1100 psia and stagnation temperatures from 660 to 1130°R.

2.2 MODELS

Two basic models (see Fig. 2) were used: a body of revolution with interchangeable noses and flares and a flat plate with a hinged, trailing-edge ramp.

The axisymmetric configurations (Fig. 2a) had a common cylinder for the interchangeable noses and flares. The cylinder section had pressure orifices (0.042 ID) spaced 0.5 in. apart starting 0.06 in. from the nose joint, whereas the three instrumented flares had the same size orifices spaced 0.25 in. apart along most of their length. These orifices were staggered along five rows each 15 deg apart. The orifice closest to the flare leading edge was 0.50 in. away on the 7.5- and 10-deg frustums and 0.30 in. on the 15-deg frustum. The flares were sealed with an O-ring between them and the cylinder. Additional flares of 2.5, 5, and 20 deg, but without orifices, were used during a preliminary investigation of the pressure distribution upstream of the flare. All configurations were sting supported and were aligned to within ±0.05 deg of parallel with the flow. Although the flare was adjustable on the cylinder, it was fixed such that $\Delta x_c = 3.8 \pm 0.05$ in. for all but a few runs. Some data for $\Delta x_c = 2.6$ in. as well as for $\Delta x_c = 3.8$ in. are presented at $M_\infty = 5$.

The ramp model (Fig. 2b) is the same one used in Ref. 5 except that 0.042-in.-ID orifices were installed along the flat plate centerline at a spacing of 0.2 in. from the hinge line to within 1.0 in. of the leading edge. End plates (Fig. 2c) were also built to check the conclusions of Ref. 8 regarding the two-dimensionality of the flow with a 9-in. span ramp. These plates, which were sealed along all edges with a silicone mastic, were screwed to the ramp edges like vertical

fins and projected well above the ramp trailing edge and upstream of the beginning of the interaction process. The model was supported on rails attached to the tunnel sidewalls, and the flat plate was aligned parallel to the flow within ±0.05 deg.

2.3 INSTRUMENTATION

The surface pressures were measured with a pressure-scanning system in Tunnel D, whereby 11 orifices may be read with either a 1- or 15-psi differential pressure transducer referenced to a near vacuum. In order to reduce small random differences in transducers, the model taps were connected in sequence to one transducer system before utilizing the next one. Frequent calibrations near the pressure level to be measured also minimized drift and nonlinearities of the transducers. Repeat runs and comparisons with the tunnel evacuated indicate that the deviations among all pressure readings were always less than ±0.002 psi in a given run.

For the tests in Tunnel E, individual 5-psid differential pressure transducers (having a variable reference pressure) were used. Repeat runs and comparison of readings with the tunnel evacuated prior to a run showed that the variation between the transducers was never more than ±0.005 psi.

The centerbody wall temperature, which was monitored during all tests, generally was near an equilibrium condition in Tunnel E being approximately 0.90 T_o at Mach 5 and 0.84 T_o at Mach 7. During the Tunnel D tests, particularly at low densities at Mach 3 or 5, the model wall temperature was usually more than 0.95 T_o.

Spark schlieren pictures in Tunnel D and spark shadowgraphs in Tunnel E were taken for each test condition.

2.4 OIL FLOW TECHNIQUE

A physical indication of the streamline direction in the boundary layer is given by the application of a thin oil film to the model surface. A flourescent penetrating oil was used here because it glows brightly against any background when lighted by an ultraviolet light. It was used primarily to locate the separation and reattachment positions on the flared cone-cylinder configurations by noting that a line of accumulation will develop at separation and a line of depletion at reattachment. The best results were obtained by painting the surface with an even coat of oil in the region slightly upstream and downstream of the expected location.

Separation was consistently easiest to define. Since these measurements were made only at Mach 3, it is not known whether the gradual cooling of the flare during a run was solely responsible for the sluggishness of the oil film observed near reattachment.

The oil film was also used to indicate streamline patterns during the end plate investigation. Examples of this are shown in Fig. 3 where the effect of end plates on the flow over the ramp (undeflected) is clearly indicated. Two bands were painted: one at the leading edge, the other at the hinge line. These pictures show that the end plates significantly improved the cross flow at the edges of the ramp without affecting the centerline flow.

SECTION III
RESULTS AND DISCUSSION

3.1 PRESSURE DISTRIBUTIONS – AXISYMMETRIC MODEL

A majority of the data obtained with the sharp, cone-cylinder-flare configurations are shown in Figs. 4 through 6, where the surface pressure coefficient is plotted against the surface distance upstream and downstream of the flare leading edge using the free-stream unit Reynolds number as the variable of interest. The data for $\theta = 7.5$ deg (Fig. 4), which are in general similar to those for the larger flare angles in Figs. 5 and 6, do exhibit an uncommon characteristic at $M_\infty = 3$ and 5 at the minimum Reynolds number. That is, within the precision of these data, no reflex in the pressure distribution at the flare leading edge is indicated. Although such distributions are quite like those found by Kuehn (Ref. 9) at the incipient separation condition, oil film measurements at $M_\infty = 3$, included in Fig. 4a, indicate that separation still exists. These oil film data will be discussed further in a later section of this report.

From a general examination of these data in Figs. 4 through 6, it may be noted that the flare pressure requires the most length to reach its peak level at low Reynolds number, and that at a given Mach number this length is fairly independent of flare angle. Besides demonstrating this latter point, Fig. 7 shows that the upstream influence increases for increasing flare angle. The effect of flare angle (overall pressure rise) upon the extent of flow separation is probably the only variable in the literature on shock-induced flow separation for which no controversy exists regarding its general influence. Despite all the experiments

and theoretical work of the past ten years, the effects of Mach number and Reynolds number upon laminar-flow-separation scaling are still unresolved even for the adiabatic wall case in uniform flow.

A majority of the data obtained with the hemisphere-cylinder-flare configurations are shown in Figs. 8 through 10, respectively, for θ = 7.5, 10, and 15 deg. Data for the 7.5-deg semi-angle flare shown in Fig. 8a indicate the absence of a definite reflex at almost all flow conditions, and only at the highest Reynolds number at $M_\infty = 3$ is a reflex in the pressure distribution clearly indicated. Although more orifices are required to verify the absence of a reflex, it should be apparent that the beginning of the interaction is fairly well represented by the fairings shown; the upstream influence could, however, be slightly less if the data were faired with a reflex curve.

With regard to the flare length required for the surface pressure to reach the inviscid level, the data of Figs. 8 through 10 indicate that it is fairly independent of Reynolds number being approximately one body diameter long for all flares tested. This is less than was found for the sharp cone configuration. The effects of flare angle at $M_\infty = 5$ and 7 are illustrated in Fig. 11 at a fixed Reynolds number. As before (in Fig. 7), increasing flare angle causes an increasing extent of separation once it occurs. In this case, however, the nonuniform inviscid flow field causes a pressure gradient along the flare, downstream of the boundary-layer interaction, which increases as flare angle is increased.

3.2 PRESSURE DISTRIBUTIONS – RAMP MODELS

The surface pressure data on the ramp model configuration, at $M_\infty = 3$, is presented in Fig. 12 as a function of unit Reynolds number for ramp angles of 7.5, 10, and 15 deg. Although these results are quite comparable to the axisymmetric data in terms of the upstream influence of a given ramp/flare angle, it is quite apparent that the unit Reynolds number at which the reflex in pressure ahead of the ramp disappears (for θ = 7.5 deg) must be appreciably lower than that for the flared configuration. This is to be expected since the peak pressure to be attained during reattachment is greater in two-dimensional flow. Since these data show that the initial pressure gradient on the ramp decreased as the unit Reynolds was decreased, it follows that lower Reynolds numbers may be required for the incipient separation condition on ramps.

These results also indicate that the length required to achieve the peak pressure is appreciably greater on the ramp than it is on the flare. Since the influence of Reynolds number on this length is similar to that shown for the flare configuration, the differences might be associated with three-dimensional effects on the shear layer growth after separation.

A most interesting pressure distribution was obtained at $Re_c = 0.205 \times 10^6$ with the 7.5-deg ramp (Fig. 13). In this case only was the reattachment (ramp) pressure gradient obviously less than that at separation. This suggests that there should be a hysteresis effect in the condition for incipient separation.

3.3 UPSTREAM INFLUENCE – AXISYMMETRIC MODELS

The distance upstream of the flare or ramp where the surface pressure first rises above that obtained in the absence of a flare or ramp is termed the upstream influence, $(x_o - x_c)/x_c$. This is the same length as first correlated by Gadd, Holder, and Regan (Ref. 6). The variation of $(x_o - x_c)/x_c$ with Reynolds number was obtained primarily from the data given in Figs. 4 through 9. Results for the cone-cylinder configuration, at fixed Mach number with the flare angle a parameter, are shown in Fig. 14. These data indicate that the effect of Reynolds number on the upstream influence is varied and significantly affected by flare angle and free-stream Mach number. In general, it may be noted that by increasing the flare angle sufficiently at any Reynolds number, the variation of upstream influence will change from an increase to a decrease in the extent for Reynolds number increasing. These curves for $\theta \leq 10$ deg illustrate a most interesting point regarding the effect of Mach number on the upstream influence - depending on the Reynolds and Mach number, the variation of upstream influence with Mach number may be increasing, decreasing, or nearly constant.

The effects of Reynolds number variation upon the upstream influence of various flares on the hemisphere-cylinder model are summarized in Fig. 15. It is noted that there is little variation with Reynolds number. Comparison of the data in Fig. 15b for $\theta = 7.5$ deg at $M_\infty = 5$, where the flow is not fully separated (see Fig. 8a and 8b) with that of $\theta = 10$ deg at $M_\infty = 5$ where the flow goes from effectively unseparated to fully separated (see Fig. 9b), indicates that the upstream influence in the absence of separation may be of the same order as when it clearly exists. It may be observed by comparisons of Figs. 14 and 15 that although there are substantial reductions in $(x_o - x_c)/x_c$ caused by

nose blunting at $M_\infty > 5$, there is very little shown for Mach 3. Furthermore, it is obvious that the upstream influence for the blunt-nose models decreases with free-stream Mach number increase, whereas an increase is shown with the conical nose between $M_\infty = 3$ and 5. The local Mach number on a hemisphere-cylinder is known to be nearly invariant (approximately M = 3.5) in the hypersonic range; therefore, these effects noted are not associated with the Mach number level at the boundary-layer edge. Indeed, the only explanation remaining is the appreciable vorticity, outside the boundary layer, produced by the bow wave curvature. Thus, the external vorticity may be coupled with the viscous vorticity to produce an effect like a substantially thickened boundary layer.

3.4 TRANSITION INFLUENCE – AXISYMMETRIC MODELS

The critical influence of transition upon the pressure distribution in separated flows, as demonstrated by Chapman, Kuehn, and Larson (Ref. 7), is a well accepted principle of fluid mechanics. Their findings, however, were based primarily upon experiments with forward and rearward facing steps which produced substantial regions of reverse flow with either reattachment or separation position being essentially fixed. Now with regard to the influence of transition on the scale of wedge-type separations, only Gadd, Holder, and Regan (Ref. 6) have specifically conducted such studies in adiabatic flow. However, Needham (Ref. 10) has recently studied this particular problem for the cold wall case in hypersonic flow. It would appear that the work of Gadd et al. has mainly been ignored, judging from the almost total lack of citations from this reference on that subject in the published literature. No doubt, the absence of any experimental pressure distributions was a substantial influence as was the anomaly in the significance ascribed to the pressure plateau between the two references (Refs. 6 and 7). Despite this situation, only in Refs. 6 and 10 was an apparent reversal in trend with Reynolds number noted for the upstream influence when the flow near reattachment changed from laminar to transitional. As noted recently in Ref. 11, confusion still exists regarding the influence of Reynolds number on the extent of wedge-type flow separations, probably because of an uncertainty in the conditions governing the existence of a substantial pressure plateau.

In order to clarify this, data are required which relate the variation of the beginning of transition to the reattachment region for the conditions which affect either of these, namely, flare angle, Mach number, and Reynolds number. The

transition data obtained from measurements of schlieren and shadowgraph pictures are shown in Fig. 16. The wetted length to transition, as measured from the position of the flare leading edge, is plotted versus Reynolds number with flare semi-angle a parameter at fixed free-stream Mach number. Typical schlieren pictures at $M_\infty = 3$ and 5 are given in Fig. 17 and shadowgraphs at $M_\infty = 5$ in Fig. 18. Arrows indicate the beginning of the upstream interaction, x_o, as determined from surface pressure distributions and the beginning of transition, x_t, as derived from several photographs for the same test conditions. It must be clearly understood that transition indications from schlieren or shadowgraph pictures are not repeatable within the precision which must be implied by the use of an arrow as in these typical photographs. Indeed, there is, in general, a band within which transition will be found from repeated photographs. In these tests, the bandwidth was never much more than about an inch. However, in all cases, the most upstream indication of the beginning of transition was consistently chosen.

An important point is indicated by the data in Fig. 16a. Namely, the increment between the indicated location of transition when $\theta \geq 0$ and when $\theta = 0$ decreases with increasing Reynolds number. Moreover, the increment over which transition moves upstream is never more than the distance from the flare leading edge to the transition location when $\theta = 0$

It also may be seen from these pictures that an estimation of the upstream influence from photographs at supersonic speeds is very difficult since there are not any separation shocks near the boundary-layer edge like those observed by Needham (Ref. 10) at $M_\infty = 9.7$.

It is apparent from these examples that transition is easier to detect via the shadowgraph technique; therefore, the differences shown for $M_\infty = 5$ in Figs. 16b and c (as obtained in Tunnels D and E) are to be expected. It is most significant, however, that the data show that the adverse pressure gradient (flare angle) is as important as the Reynolds number in controlling the onset of transition. No transition data are presented for the hemisphere nose configurations since few pictures gave any indication of the transition process. This is not too surprising since the local density and density gradients are especially reduced by the bow wave vorticity near the boundary-layer edge.

In the absence of complete oil film data, the location of flow reattachment, $(x_m - x_c)/x_c$, has been defined as shown in the accompanying sketch, i.e. midway in the flare pressure rise. Holden (Ref. 12) has indicated that it is no further

upstream than this; thus, such location should be reasonably conservative. Having determined $(x_o - x_c)/x_c$ and $(x_m - x_c)/x_c$ from the surface pressure distributions, and $(x_t - x_c)/x_c$ from schlieren and shadow photographs taken during the pressure measurements, the dependence of upstream influence on the relative location of transition may be shown. This is done in Fig. 19 by plotting $(x_o - x_c)/x_c$ and $(x_t - x_m)/x_c$ each versus Reynolds number for a fixed flare angle with Mach number a parameter.

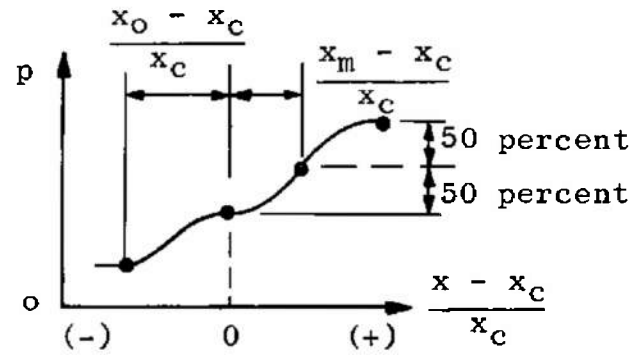

These curves shown that when $(x_t - x_m)/x_c >> 0$, the upstream influence grows with increasing Reynolds number, whereas when $(x_t - x_m)/x_c$ approaches zero and becomes negative, the upstream influence reaches a maximum and then decreases with increasing Reynolds number. Potter and Whitfield (Ref. 13) have shown that transition indications from conventional schlieren are consistently well downstream of the actual beginning of laminar flow. In fact, their data show that the absolute difference might be as large as 0.30 for $M_\infty = 3$ at $Re_c = 1.34 \times 10^6$ and almost double that at Mach 5. Accordingly, the curves of critical transition increment based upon schlieren data have been shifted as indicated in Figs. 19a and b by solid symbols for $\theta = 7.5$ and 10 deg.

It must be emphasized that these corrections are based upon transition data for which the pressure gradient was zero. Indeed it appears that in this case of nonzero pressure gradients, the true correction may be less than that applied. Specifically, the data in Fig. 19b for Mach 3 indicate that transition would be about 0.15 upstream of $(x_m - x_c)/x_c$, and from the pressure data in Fig. 5a, it may be seen that this would require transition to be upstream of the flare leading edge. Results in Ref. 7 show that whenever transition is well upstream of reattachment (prior to the final pressure rise) the onset of transition will significantly influence the surface pressure distribution. Therefore, the absence of such evidence in Fig. 5a indicates that transition was not upstream of the flare and that the length of the transition zone may be reduced by the action of an adverse pressure gradient. The shift of the data shown obviously renders the data at the lower end of Reynolds number more consistent with the shadowgraph-based data.

The data at Mach 5 and 7 in Figs. 19a and b are particularly clear evidence of a reveral in the growth of the upstream influence with Reynolds number. The data for $\theta = 15$ deg (Fig. 19c) are especially conclusive evidence of the characteristic effect of Reynolds number on the upstream influence (or scale of separation) when transition begins upstream of flow reattachment; that is, when $(x_t - x_m)/x_c < 0$. The data for which flow reattachment was laminar, $(x_t - x_m)/x_c >> 0$, indicate that for a given flare the increase of separation extent with Reynolds number increase grows with Mach number in the supersonic range and may decline some at hypersonic speeds. Moreover, a flare angle increase at a particular Mach number also magnifies the increase of separation with Reynolds number increase. Therefore, it is not surprising that the data of Ginoux at $M_\infty = 2$ for 5- and 7-deg ramps (Ref. 4) showed almost negligible variation, and that Needham's data (Ref. 10) at $M_\infty = 9.7$ for a 13-deg ramp showed that the upstream influence clearly increased with Reynolds number increase.

3.5 TRANSITION INFLUENCE – RAMP MODELS

Transition data for the ramp configuration at $M_\infty = 3$ are given in Fig. 20 for various ramp angles as determined from schlieren photographs. These data, however, show that transition began much further upstream on the flat plate than on the cone cylinder. This, therefore, makes the ramp model less satisfactory since it decreases the range of Re/in. available for studying the scaling of separation extent of flows which remain laminar through reattachment.

The reattachment transition increment $(x_t - x_m)/x_c$ for the ramp model is shown in Fig. 21. It is shown as derived from schlieren data as well as when shifted upstream 0.53 for the reasons discussed in Section 3.4. Similarly, these data indicate that the correction is overdone since no evidence of transition influences of the surface pressure distribution upstream of the ram exists in Fig. 12. Nevertheless, these data similarly indicate that transition upstream of the reattachment zone causes the upstream influence (extent of separation) to decline as Reynolds number is increased. By referring back to the pressure data, it may be noted that no plateau exists for $\theta = 7.5$ deg (Fig. 12a), whereas one does indeed for $\theta = 15$ deg at the minimum Reynolds number (Fig. 12c). Since these data are classified as transitional-type flow separations, this demonstrates that the absence of a pressure plateau is not intrinsic evidence of the existence of laminar-flow reattachment.

3.6 OIL FILM DATA – AXISYMMETRIC MODELS

Some representative oil film pictures before and after runs at $M_\infty = 3$ are presented in Fig. 22. The pictures are presented to show the influence of flare angle on the oil film patterns at $Re_c = 0.36 \times 10^6$ as well as give some indication of the quality of data derived from these tests. In order to show a rather typical reattachment phenomenon for the larger flares ($\theta \geq 7.5$ deg), an enlargement of the oil film data for $Re_c = 0.90 \times 10^6$ with a 10-deg flare is given in Fig. 23. Considerable care was taken to be sure that the model was aligned with the flow, for when it was off by as little as 0.1 deg, the separation or reattachment could become skewed. Therefore, this effect is not believed to be caused by crossflow over the model, although it is quite similar to one of the vortex striations shown by Thomke (Ref. 14) for turbulent reattaching flows.

The measurements of separation and reattachment are summarized in Fig. 24 to indicate the effects of Reynolds number variation holding flare angle constant. These data for $\theta \leq 10$ deg indicate that both the separation and reattachment locations move away from the flare leading edge for increasing Reynolds number when $Re_c \leq 0.93 \times 10^6$, whereas the opposite effect is shown for $\theta = 20$ deg. This is generally consistent with the trends already observed in Fig. 19 for the upstream influence and shown to be caused by the movement of transition upstream of the midpoint of the flare pressure rise.

Another interesting comparison is provided by the tick marks added to the pressure distributions for $\theta = 7.5$ and 10 deg in Figs. 4a and 5a. These marks which represent the corresponding oil film data for separation and reattachment from Fig. 24 are particularly surprising because they are both so much closer to the beginning and end of the interaction zone than was expected on the basis of two-dimensional studies in Ref. 7 and 12. In fact, they indicate that separation exists where the pressure gradient first reaches a maximum, rather than later on where the pressure rise is about one-half of the rise to the reflex in the distribution (at the corner). These marks also suggest that reattachment is located at the end of the maximum pressure gradient, that is where the flare pressure gradient first begins to decline. This is significantly different from the locations found by Thomke (Ref. 14) in turbulent reattaching base flows; his data show that flow reversal occurred near the midpoint of the recompression.

3.7 SEPARATION PRESSURE GRADIENT

The pressure gradient at separation which is determined by an interaction between the boundary layer and the local external flow must also be the critical value required of a deflected surface for flow separation to first occur. Therefore, an understanding of the influence of Reynolds and Mach number on the separation gradient should clarify the conditions governing incipient separation. This general situation is perhaps better illustrated by the accompanying sketch of pressure distributions for increasing Reynolds number. At a sufficiently low Reynolds number, ①, the pressure gradient is less than the critical value, ②; thus, most of the pressure rise to the peak level takes place on the ramp. Furthermore, Reynolds number increase beyond the incipient separation condition, ②, causes the ramp pressure gradient to increase and the beginning of interaction to move upstream as for ③. Finally, the Reynolds increase becomes sufficient to move transition upstream into the reattachment region, like ④. At this time, the pressure plateau is believed to first appear because the allowable reattachment pressure gradient is simultaneously increased by the thinning boundary layer and by the changing velocity profile. Thus, by far, the predominant part of the overall pressure rise is now attained on the ramp. Now, however, the beginning of the interaction process moves back downstream since less pressure rise is required upstream of the ramp. When the Reynolds number is high enough for transition to exist well upstream of the ramp, ⑤, negligible separation (if any at all) will exist. This pressure gradient, ⑤, will, therefore, be drastically larger than any previously found upstream of the ramp.

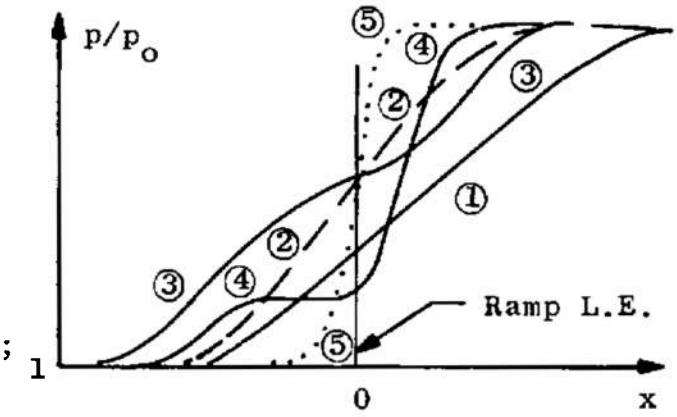

The boundary-layer momentum equation applied at the wall is given by

$$\frac{dp}{dx} = \left(\frac{\partial \tau}{\partial y}\right)_w$$

and following Chapman (Ref. 7), we assume that the wall shear gradient is proportional to the ratio of the local shear stress to the boundary-layer thickness at the beginning of

the interaction. Thus

$$(dp/dx)_s \sim \left(\frac{\tau}{\delta}\right)_o$$

Now from laminar boundary solutions (like Van Driest in Ref. 15) we may write

$$\left(\frac{\tau}{\delta}\right)_o = \frac{\left[c_f \sqrt{Re}\right]_o}{\left[(\delta/x)\sqrt{Re}\right]_o} \frac{q_o}{x_o} = \left[\frac{c_f}{(\delta/x)}\right]_o \frac{\gamma}{2} \frac{p_o M_o^2}{x_o}$$

Therefore, the nondimensional pressure gradient at separation should be approximately

$$\left(\frac{dp/p_o}{dx}\right)_s x_o \sim \left[\frac{c_f}{(\delta/x)}\right]_o \frac{\gamma}{2} M_o^2$$

or in coefficient form it becomes

$$\left(\frac{dC_p}{dx}\right)_s x_o \sim \left[\frac{c_f}{(\delta/x)}\right]_o$$

Since the laminar boundary-layer skin friction and thickness parameters ($c_f \sqrt{Re}$ and $\delta/x \sqrt{Re}$, respectively) are only functions of Mach number and wall temperature, the pressure gradient, $d(p/p_o)/dx$, at separation is only a function of the length to the beginning of the interaction, the local Mach number, and the heat transfer.

Some experimental results for the separation pressure gradient are compared in Fig. 25 with the theoretical function just derived. Two-dimensional data of Chapman, Kuehn, and Larsen, as well as data from Fig. 12, are in good agreement with this laminar boundary-layer parameter for an insulated (adiabatic) wall. The influence of heat transfer to the wall is indicated in Fig. 26 where the parameter is extended to $M_\infty = 20$ for an insulated wall and for $T_w/T_o = 0.25$. The available experimental data at higher Mach numbers suggest that wall cooling drastically changes the similarity between $(\partial\tau/\partial y)_w$, skin friction, and boundary-layer thickness. Based upon these results, it is obvious that incipient separation criteria may be appreciably different because of heat transfer.

3.8 SCALING OF SEPARATION EXTENT

Despite the obvious importance to full scale vehicles, there have been only a few reports which have dealt with the problem of scaling. Gadd, Holder, and Regan (Ref. 6) found that for ramps the upstream influence was a function of the ramp pressure coefficient and both the displacement thickness and the Reynolds number at the beginning of interaction when

the boundary layer was laminar at separation. Furthermore, it was shown that when a pressure plateau existed, the ratio of upstream influence to displacement thickness varied inversely with Reynolds number, whereas when the plateau was absent the reverse variation was observed.

In 1961, Erdos and Pallone (Ref. 16) examined existing data and proposed a correlation in terms of the dividing streamline length divided by the boundary-layer thickness at the start of the interaction. This ratio for laminar separated flows was essentially independent of Reynolds number since it is primarily a function of a pressure-rise ratio. Their flow model, however, was restricted to one having a pressure plateau.

In 1964, a new correlation of experimental results obtained with large axisymmetric models was published in Ref. 3. The basic advantage of that correlation was that the upstream influence was clearly related to the boundary-layer thickness at the flare, not to the conditions at an unknown position upstream. It was indicated that the correlation is restricted to those separations which exhibit well-developed pressure plateaus; therefore, it is obviously not valid for flows which remain laminar through reattachment. It can be shown that the correlation constants of Ref. 3 are achieved only when a plot of $(x_o - x_c)/x_c$ versus Reynolds number is concave (downward), like that for $\theta = 20$ deg in Fig. 14a. Consequently, it is seen that it would not successfully correlate much of the data of this investigation. It also can be shown that the correlation of Erdos and Pallone exhibits this same trend.

We will now rewrite the correlation parameter of Gadd et al. to compare their trends with the present results. It is shown in Ref. 6 that

$$\frac{(x_c - x_o)}{\delta_o^*} = f(C_p)_{ramp} \, Re_o^{3/4}$$

for laminar reattaching flows. Since the displacement thickness in laminar flow at adiabatic conditions is given by

$$\delta_o^* = f(M_o) \sqrt{\frac{x_o}{Re/in.}}$$

and we note that

$$x_o = x_c \left[1 + (x_o - x_c)/x_c\right]$$

finally we obtain the expression

$$\frac{(x_o - x_c)/x_c}{\left[1 + (x_o - x_c)/x_c\right]^{5/4}} = f(M_o) \cdot f(C_p)_{ramp} \cdot Re_c^{1/4}$$

which shows that the relative upstream influence, $(x_o - x_c)/x_c$,

increases roughly as the 1/4-power of Reynolds number based on the plate length, x_c. Whereas, for a fixed value of Re_c, the upstream influence, $(x_o - x_c)$, should change in proportion to plate length.

The laminar reattachment data at $M_\infty = 5$ (from Fig. 19a and b) were converted to the function on the left side of the last equation given above and were plotted versus Re_c on log-log paper to evaluate the exponent of Reynolds number. It was found that the exponent varied from 1/2 to almost zero, which is consistent with the general trends observed in Fig. 19 using more straightforward coordinates. Although this comparison further verifies the general conclusions of Ref. 6, it also indicates that the correlation found for two-dimensional flows is not applicable to axisymmetric separated flows.

In summary, it appears that of all the experimental investigations of wedge-type separations, only Gadd, Holder, and Regan's work adequately demonstrated the Reynolds number effect on the upstream influence. For inasmuch as the present results indicate the considerable ease with which transition is prematurely initiated by the adverse pressure gradient, it is indeed uncertain whether there are any pressure data in the literature for laminar reattaching flows over ramps in adiabatic, supersonic flow. It is possible that the data of Ginoux (Ref. 4) are the only pressure data which are now available, but the absence of the characteristic Reynolds number effect on the upstream influence does justify reservations.

Since there is general agreement that the stability of a separated, laminar mixing layer increases significantly with Mach number, it is somewhat surprising that there are so few published data from hypersonic facilities which show the laminar trends. Perhaps the only set of pressure data are those of Miller, Hijman, and Childs (Ref. 17) which were obtained at Mach 16. These data show a very large effect of Reynolds number upon the upstream influence. Recently, Needham (Ref. 10) published some Mach 9.7 schlieren photographs which indicate only a small increase in upstream influence with Reynolds number. Thus, there still remains a valid question concerning the effects of Mach number and Reynolds number upon separation, neither of which have been adequately investigated in adiabatic flow.

Finally, it is indicated that even the laminar theory of Lees and Reeves (Ref. 18) should be re-examined since they showed excellent agreement with data of Chapman, Kuehn, and Larson. These data show that the upstream influence decreases with Reynolds number increase, a trend shown herein to be clearly characteristic of transitional reattaching flow.

SECTION IV
CONCLUDING REMARKS

The results of this experimental investigation show that transition was always triggered prematurely by the adverse pressure gradient during laminar-flow reattachment in supersonic and hypersonic flows. Furthermore, flares of 10 deg (semi-angle) or less are required for the investigation of wedge-type separations which will remain laminar during reattachment at moderate supersonic speeds and at moderate to low Reynolds numbers. Even smaller ramp angles are required for corresponding two-dimensional studies.

General agreement with the conclusions of Gadd, Holder, and Regan was found regarding both (1) the characteristic absence of a substantial pressure plateau in the presence of laminar-flow reattachment and (2) the increase of the upstream influence when increasing the Reynolds number as long as laminar flow prevails through reattachment. Both conditions are indicated to be necessary for realization of laminar reattachment at supersonic and moderate hypersonic speeds.

Oil film data, which are believed to indicate three-dimensional effects, show that both separation and reattachment are located much nearer the beginning and end of these regions than in two-dimensional studies. Moreover, the absence of a significant reflex in the pressure rise at the flare does not correspond to the absence of flow separation.

Nose blunting was found to reduce the upstream influence of all flares for laminar reattaching flows because of the additional vorticity outside the boundary layer.

A correlation of the separation pressure gradient shows that wall cooling can produce significant increases, thereby, suggesting that incipient separation criteria may be sensitive to heat-transfer effects. Significant three-dimensional effects on incipient separation are also indicated by differences in flat plate and axisymmetric data.

Additional two-dimensional experiments on wedge-type flow separations are required because there are no data available for adiabatic, supersonic flow which are demonstratably laminar through reattachment.

REFERENCES

1. Nielsen, J. N., Lynes, L. L., and Goodwin, F. K. "Calculation of Laminar Separation with Free Interaction by the Method of Integral Relations." AFFDL-TR-65-107, June 1965.

2. Abbott, D. E., Holt, M., and Nielsen, J. N. "Investigation of Hypersonic Flow Separation and Its Effects on Aerodynamic Control Characteristics." ASD-TDR-62-963, November 1962.

3. Gray, J. D. "Laminar Boundary-Layer Separation on Flared Bodies at Supersonic and Hypersonic Speeds." AEDC-TDR-64-277 (AD609841), January 1965.

4. Ginoux, J. J. "Laminar Separation in Supersonic Flow." Final Report Contract AF EOAR 64-7, October 1964.

5. Ginoux, J. J. "Investigation of Flow Separation over Ramps at $M_\infty = 3$." AEDC-TR-65-273 (AD475242), December 1965.

6. Gadd, G. E., Holder, D. W., and Regan, J. D. "An Experimental Investigation of the Interaction between Shock Waves and Boundary Layers." Proceedings of Royal Society of London, Series A, 1954.

7. Chapman, D. R., Kuehn, D. M., and Larson, H. K. "Investigation of Separated Flows in Supersonic and Subsonic Streams with Emphasis on the Effects of Transition." NACA TN 3869, March 1957.

8. Pate, S. R. "Investigation of Flow Separation on a Two-Dimensional Flat Plate Having a Variable-Span Trailing Edge Flap at $M_\infty = 3$ and 5." AEDC-TDR-64-14 (AD432831), March 1964.

9. Kuehn, D. M. "Laminar Boundary-Layer Separation Induced by Flares on Cylinders at Zero Angle of Attack." NASA TR-R-146, June 1962.

10. Needham, D. A. "Laminar Separation in Hypersonic Flow." Ph.D. Thesis, University of London, August 1965.

11. Gray, J. D. "On the Existence of a Pressure Plateau in Pure Laminar Separated Flows." AIAA Journal, Vol. 4, August 1966.

12. Holden, M. "An Analytical Study of Separated Flows Induced by Shock Wave-Boundary Layer Interaction." CAL R-AI-1972-A-3, December 1965.

13. Potter, J. L. and Whitfield, J. D. "Effects of Unit Reynolds Number, Nose Bluntness, and Roughness on Boundary-Layer Transition." AEDC-TR-60-5 (AD234478), March 1960.

14. Thomke, G. J. "Separation and Reattachment of Supersonic Turbulent Boundary Layer behind Downstream Facing Steps and over Cavities." Douglas R SM-43062, March 1964.

15. Van Driest, E. R. "Investigation of Laminar Boundary Layer in Compressible Fluids Using the Crocco Method." NACA TN 2597, January 1962.

16. Erdos, J. and Pallone, A. "Shock-Boundary Layer Interaction and Flow Separation." AVCO RAD TR-61-23, August 1961.

17. Miller, D. S., Hijman, R., and Childs, M. E. "Mach 8 to 22 Studies of Flow Separations Due to Deflected Control Surfaces." AIAA Journal, Vol. 2, February 1964.

18. Lees, L. and Reeves, B. L. "Supersonic Separated and Reattaching Laminar Flows: I. General Theory and Application to Adiabatic Boundary Layer/Shock-Wave Interactions." AIAA Journal, November 1964.

19. Townsend, J. C., "Effects of Leading Edge Bluntness and Ramp Deflection Angle on Laminar Boundary-Layer Separation in Hypersonic Flow," NASA TN D-3290, November 1965.

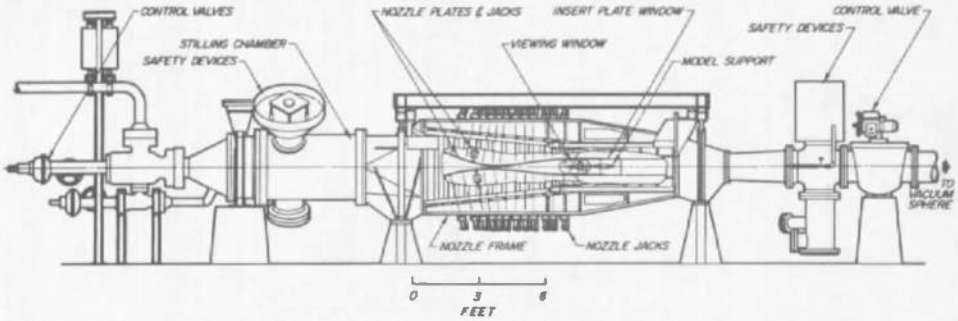

a. Tunnel D

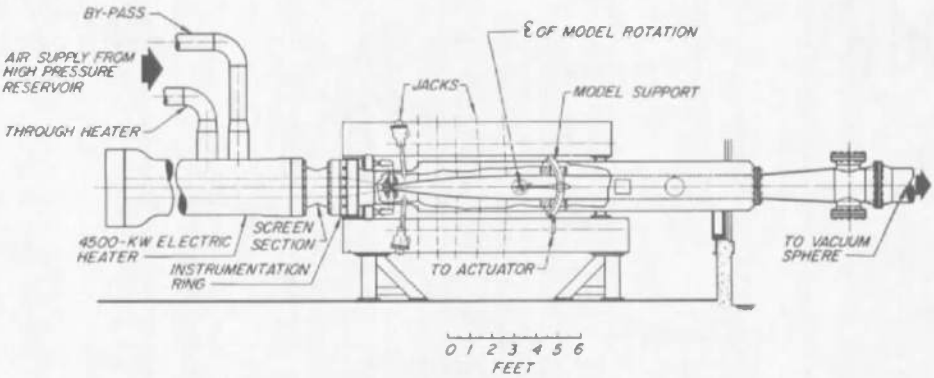

b. Tunnel E

Fig. 1 Test Facilities

NOTE: All dimensions are inches unless otherwise indicated.

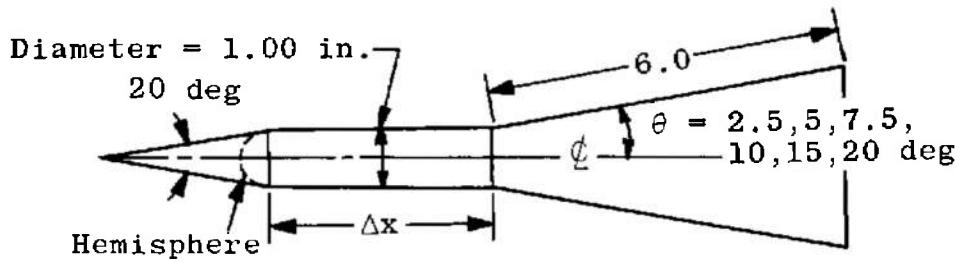

a. Flared Bodies of Revolution

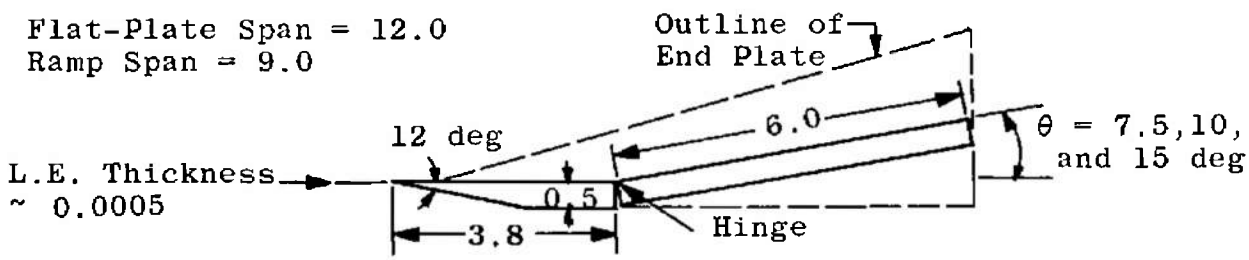

b. Flat-Plate Ramp Model

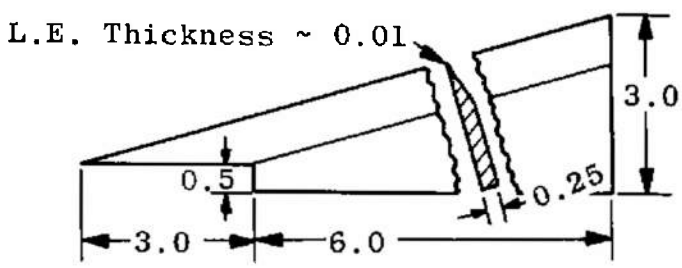

c. End Plate

Fig. 2 Model Configurations

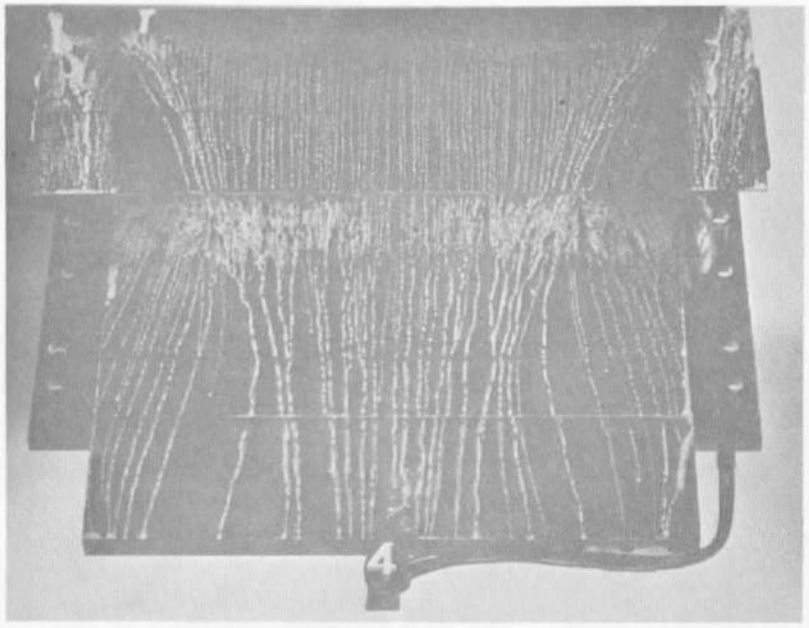

a. Without End Plates

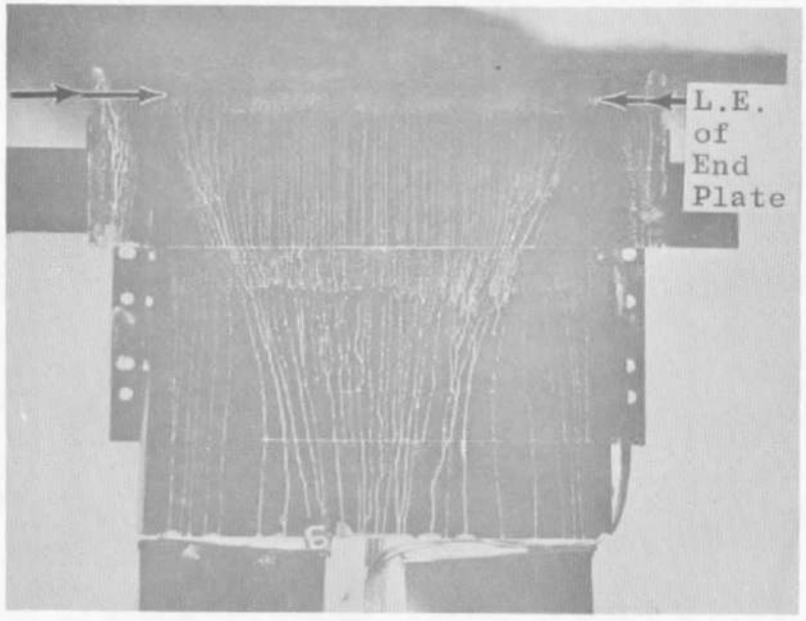

b. With End Plates

Fig. 3 Effect of End Plates on Flow at $M_\infty = 3, \theta = 0,$ $Re_c = 0.19 \times 10^6$

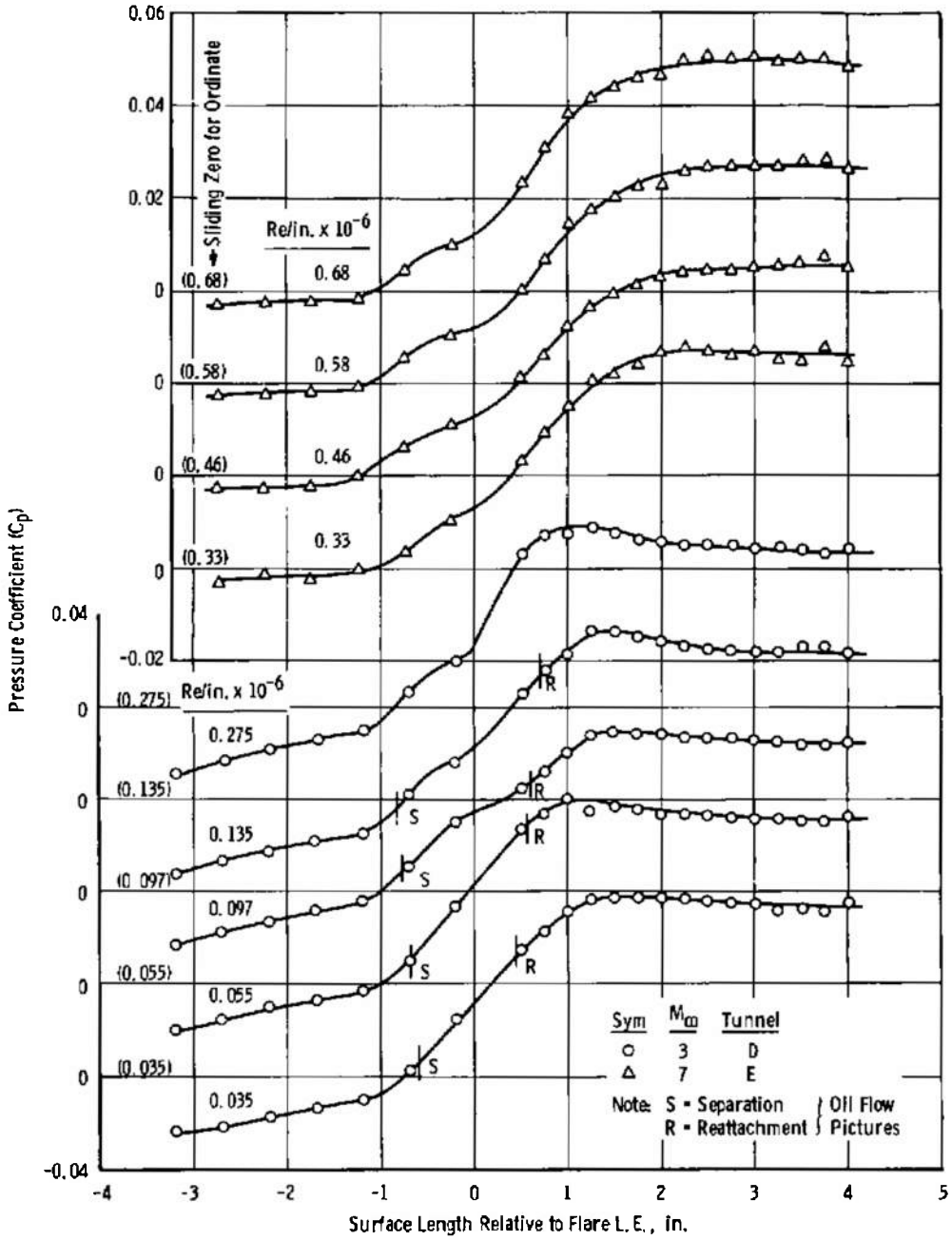

a. M_∞ = 3 and 7

Fig. 4 Pressure Distributions for Sharp Cone Model, θ = 7.5 deg, Δx_c = 3.8 in.

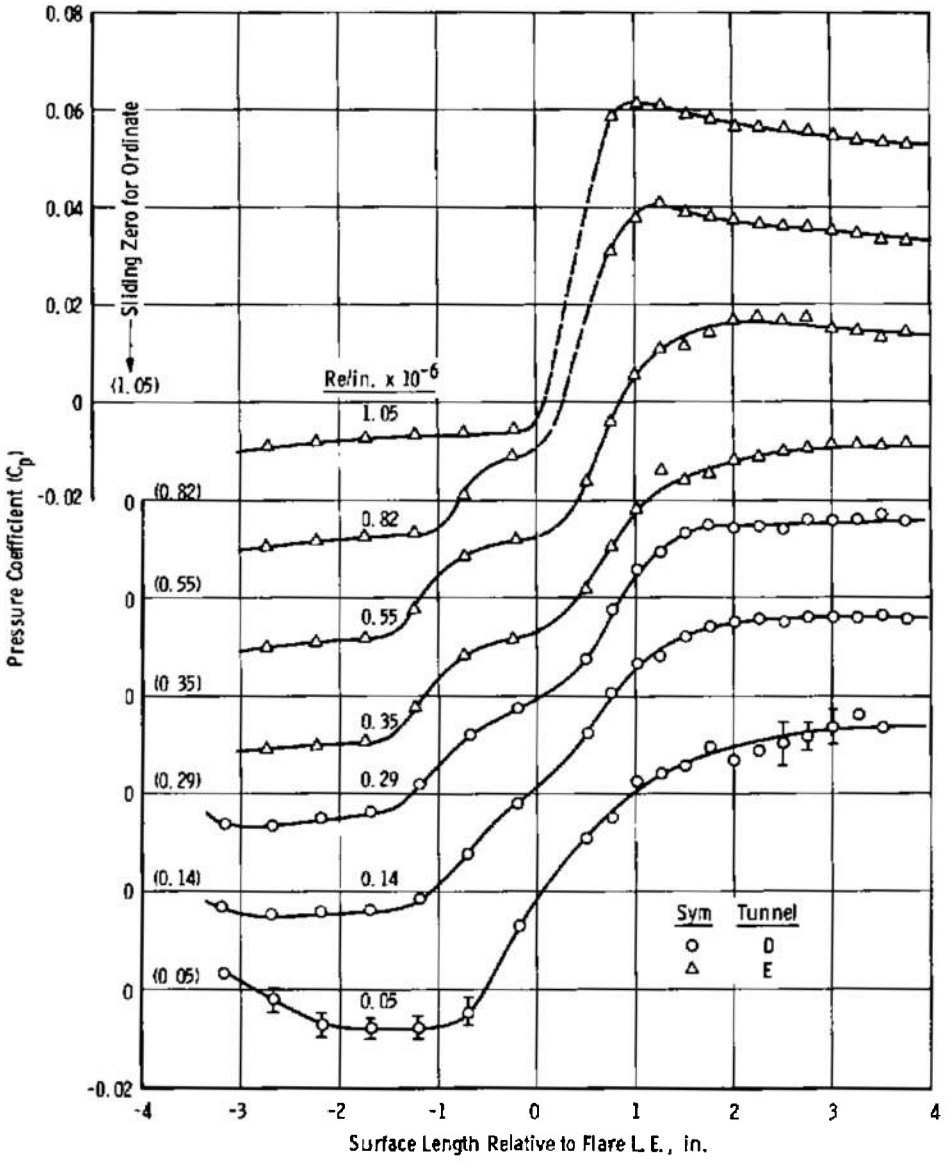

b. $M_\infty = 5$

Fig. 4 Concluded

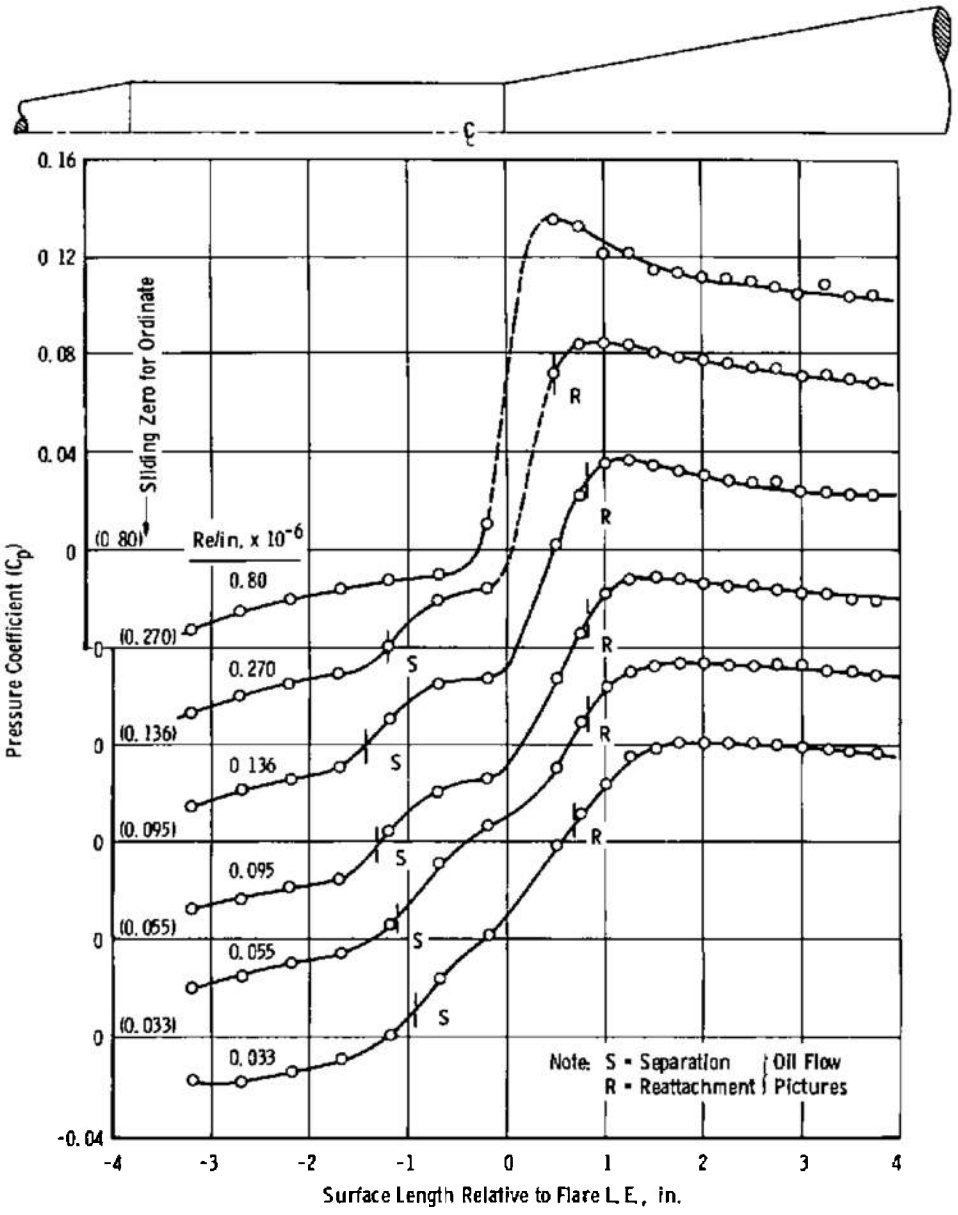

a. $M_\infty = 3$

Fig. 5 Pressure Distributions for Sharp Cone Model, θ = 10 deg, Δx_c = 3.8 in.

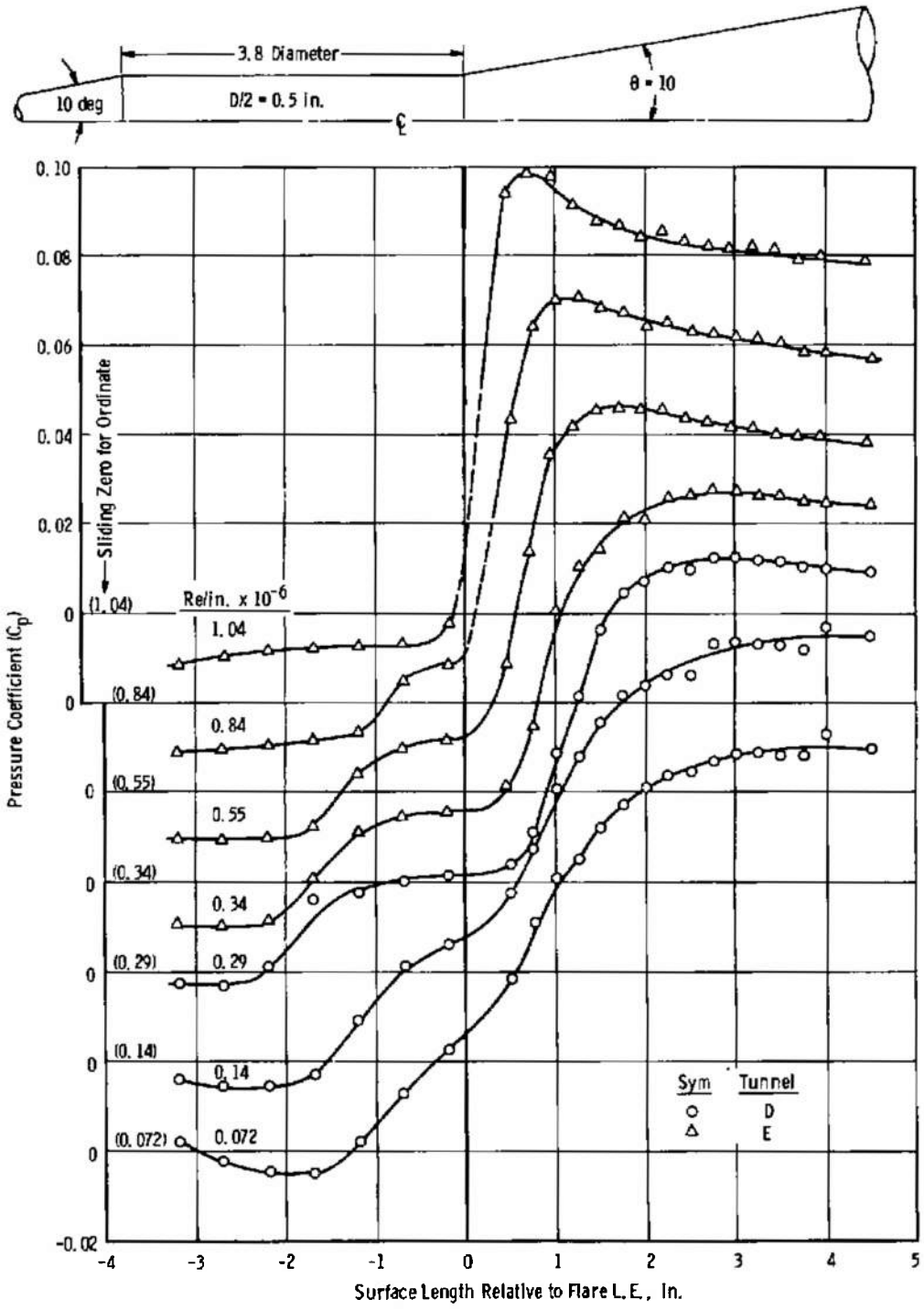

b. $M_\infty = 5$

Fig. 5 Continued

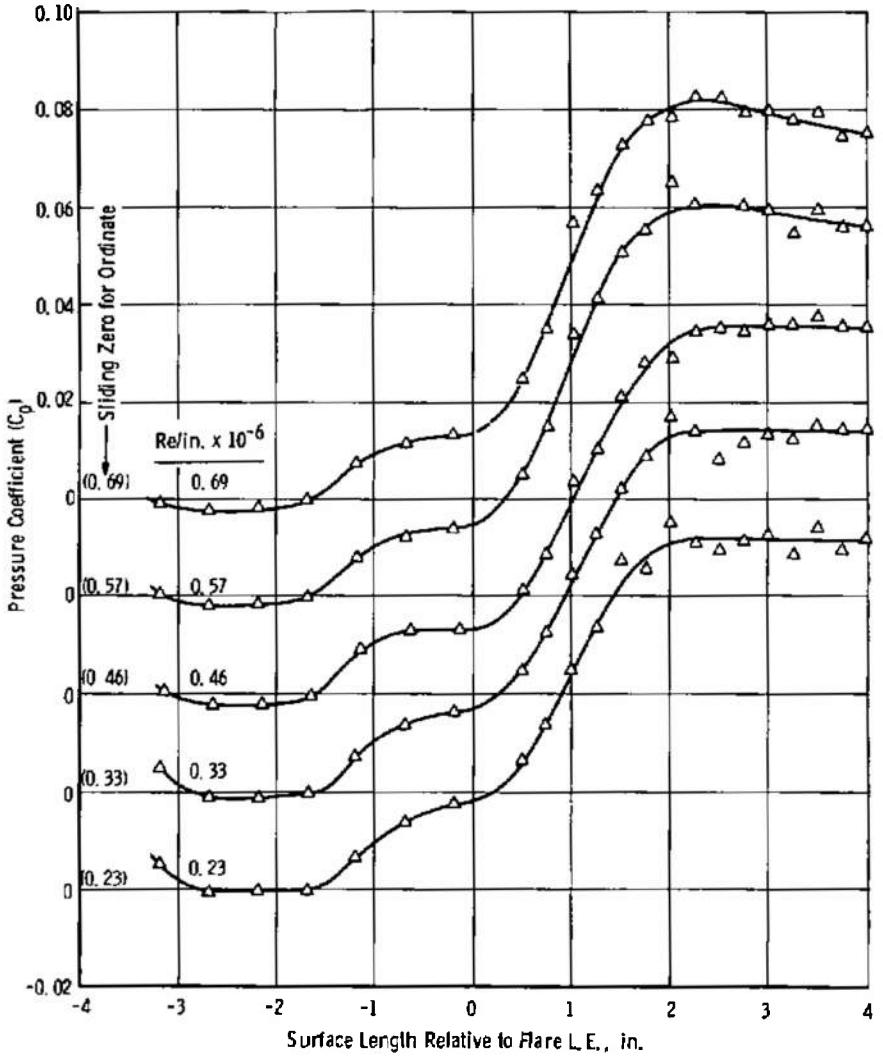

c. $M_\infty = 7$

Fig. 5 Concluded

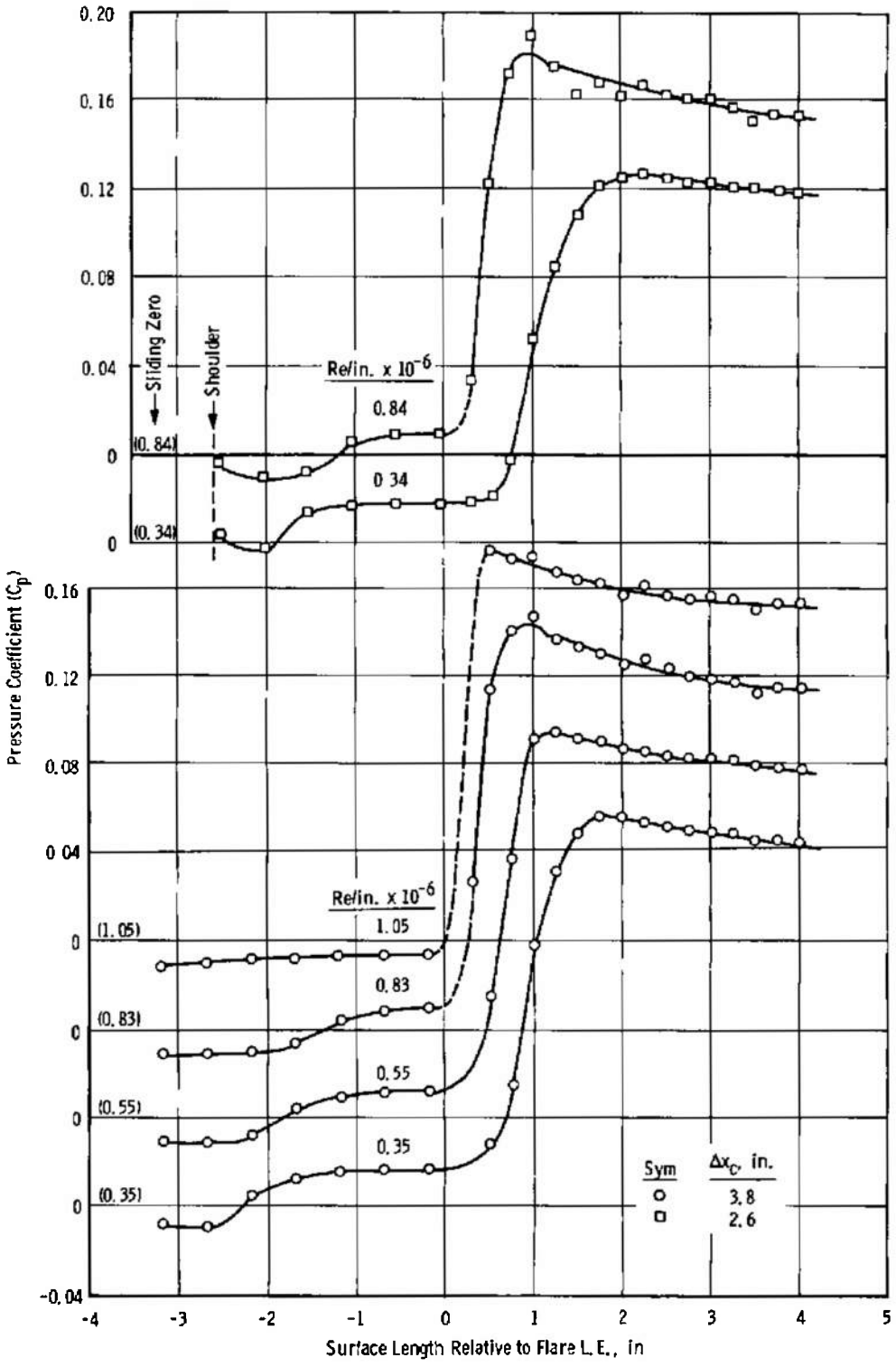

a. $M_\infty = 5$, $\Delta x_c = 2.6$ and 3.8 in.

Fig. 6 Pressure Distributions for Sharp Cone Model, $\theta = 15$ deg

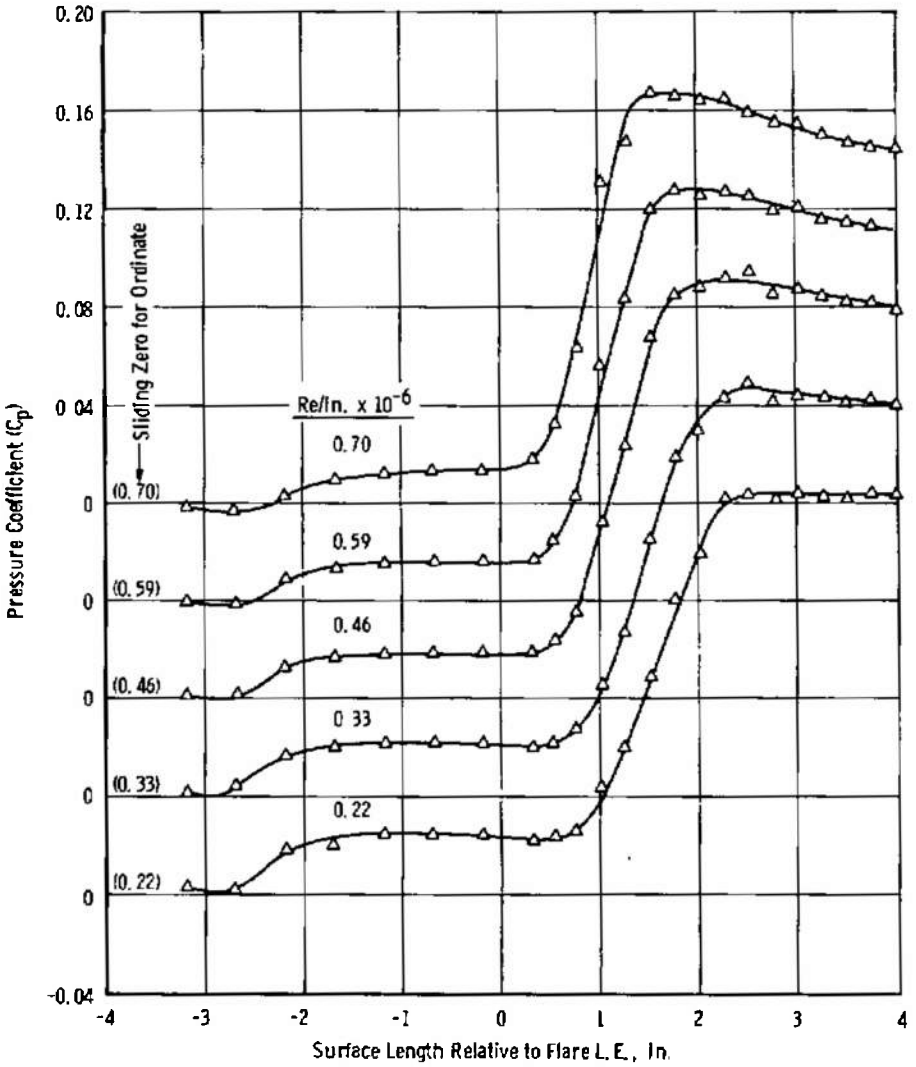

b. $M_\infty = 7$, $\Delta x_c = 3.8$ in.

Fig. 6 Concluded

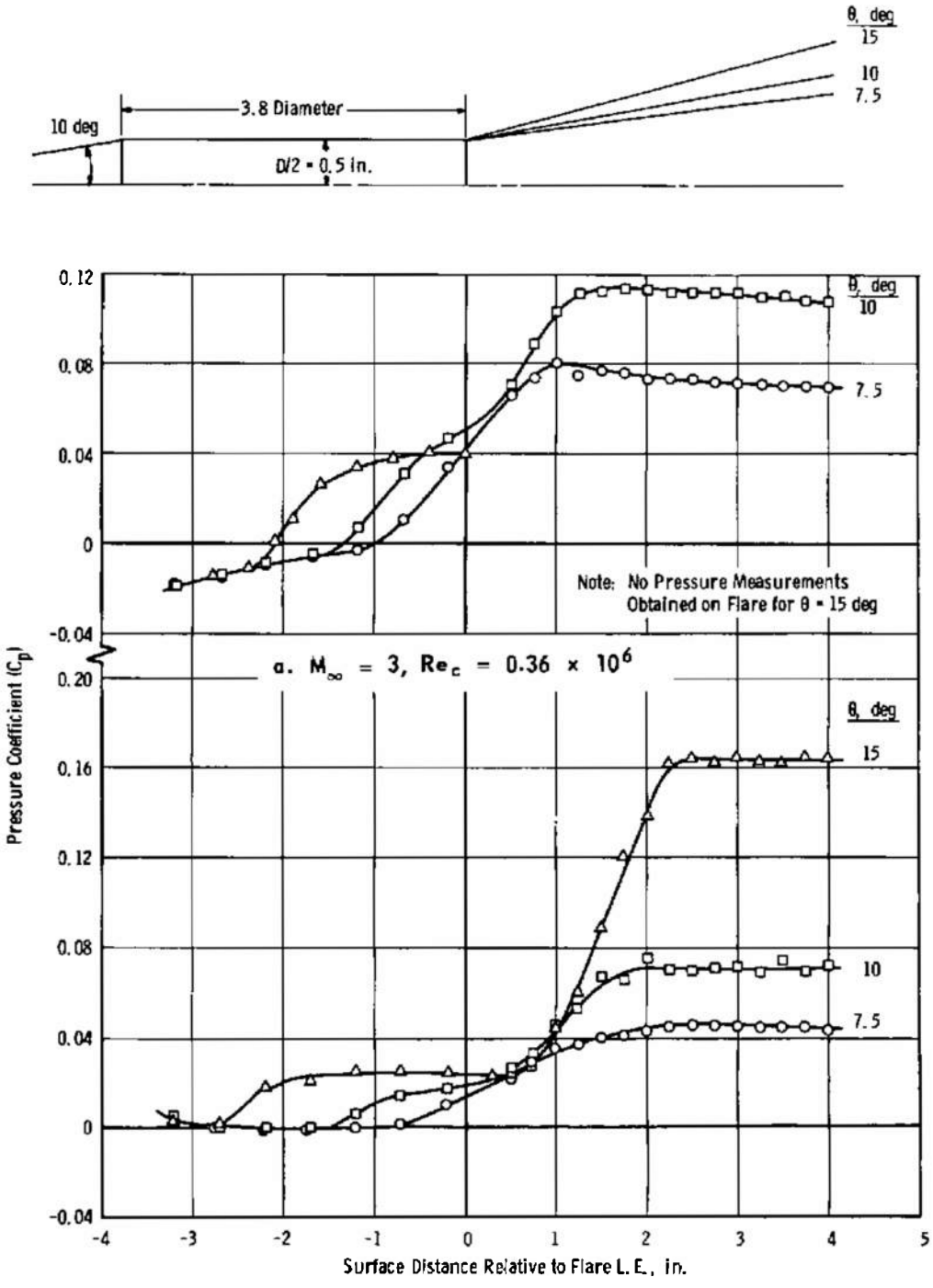

b. M_∞ = 7, Re_c = 1.47 x 10^6

Fig. 7 Effect of Flare Angle on Pressure Distribution for Sharp Cone Model

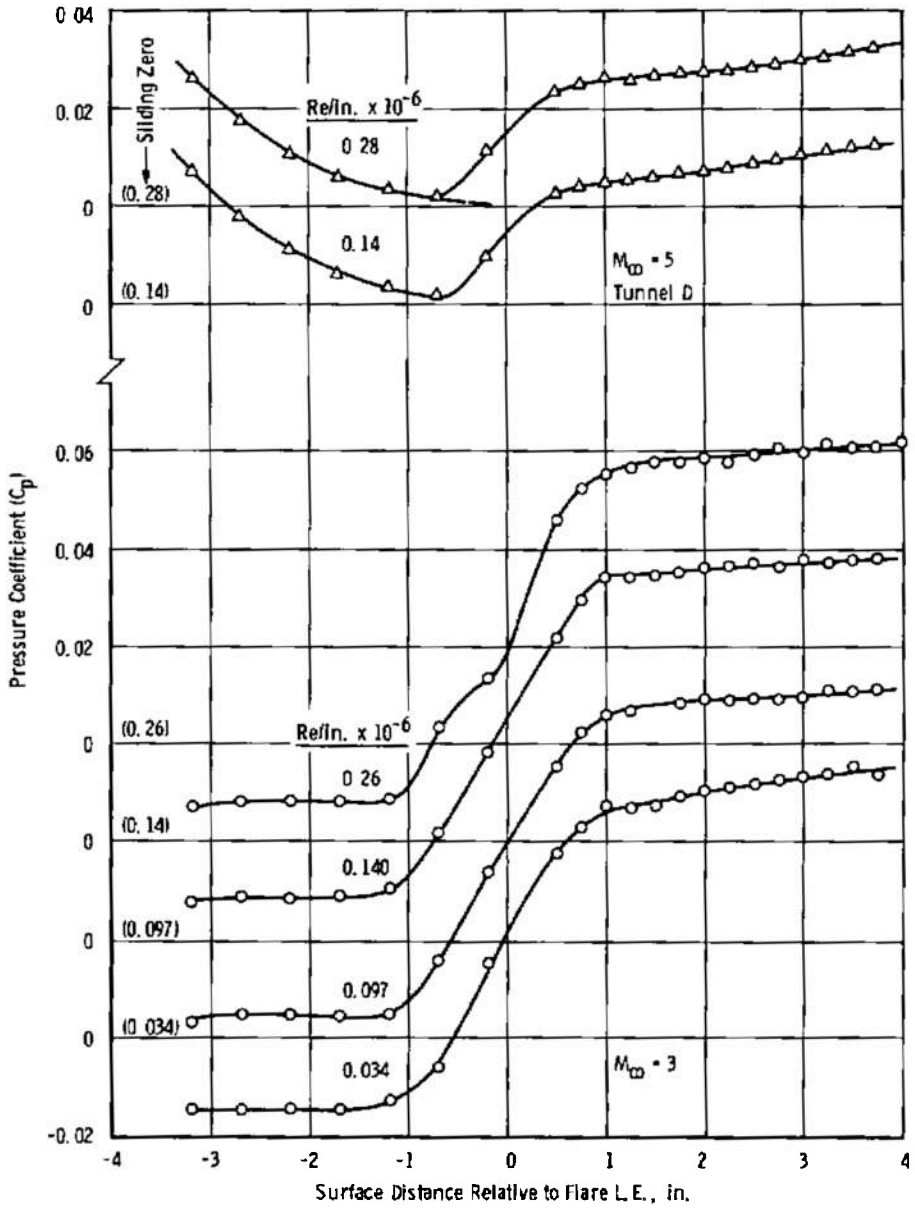

a. M_∞ = 3 and 5

Fig. 8 Pressure Distribution for Hemisphere Model, θ = 7.5 deg, Δx_c = 3.8 in.

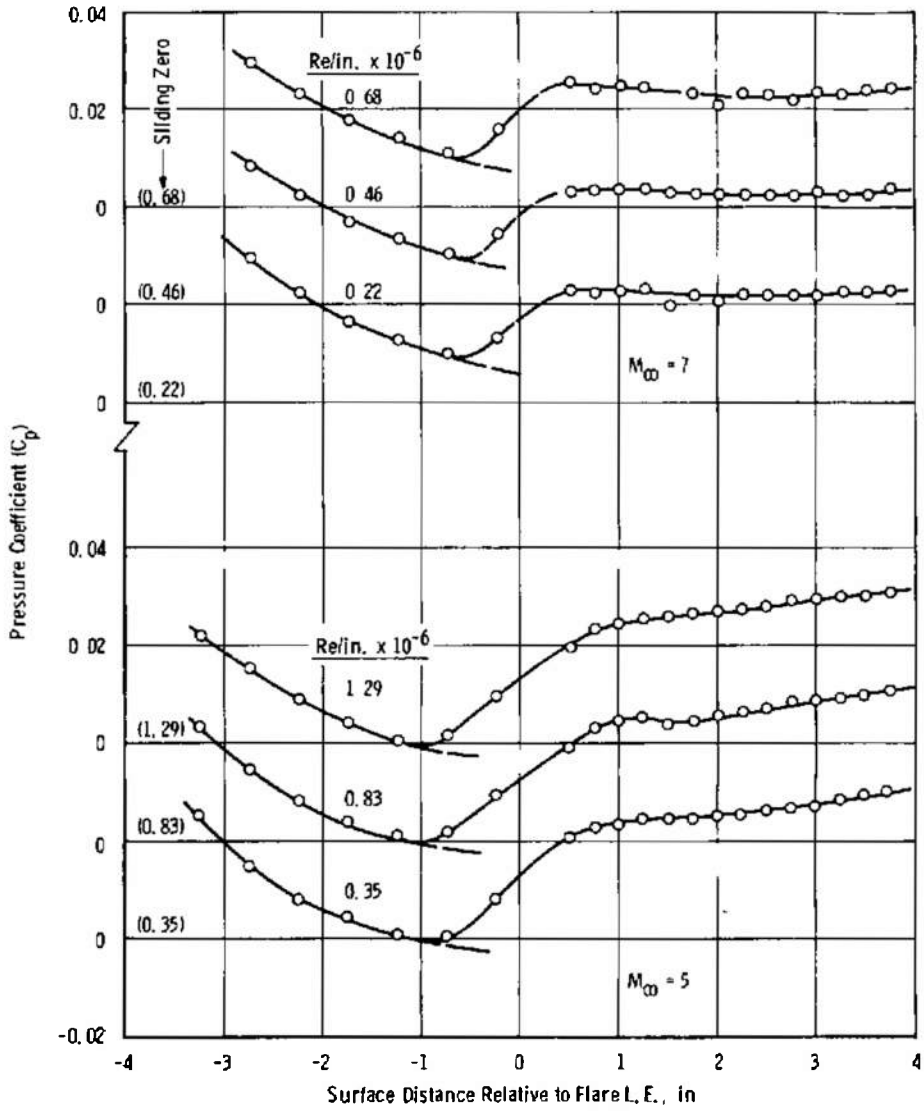

b. M_∞ = 5 and 7

Fig. 8 Concluded

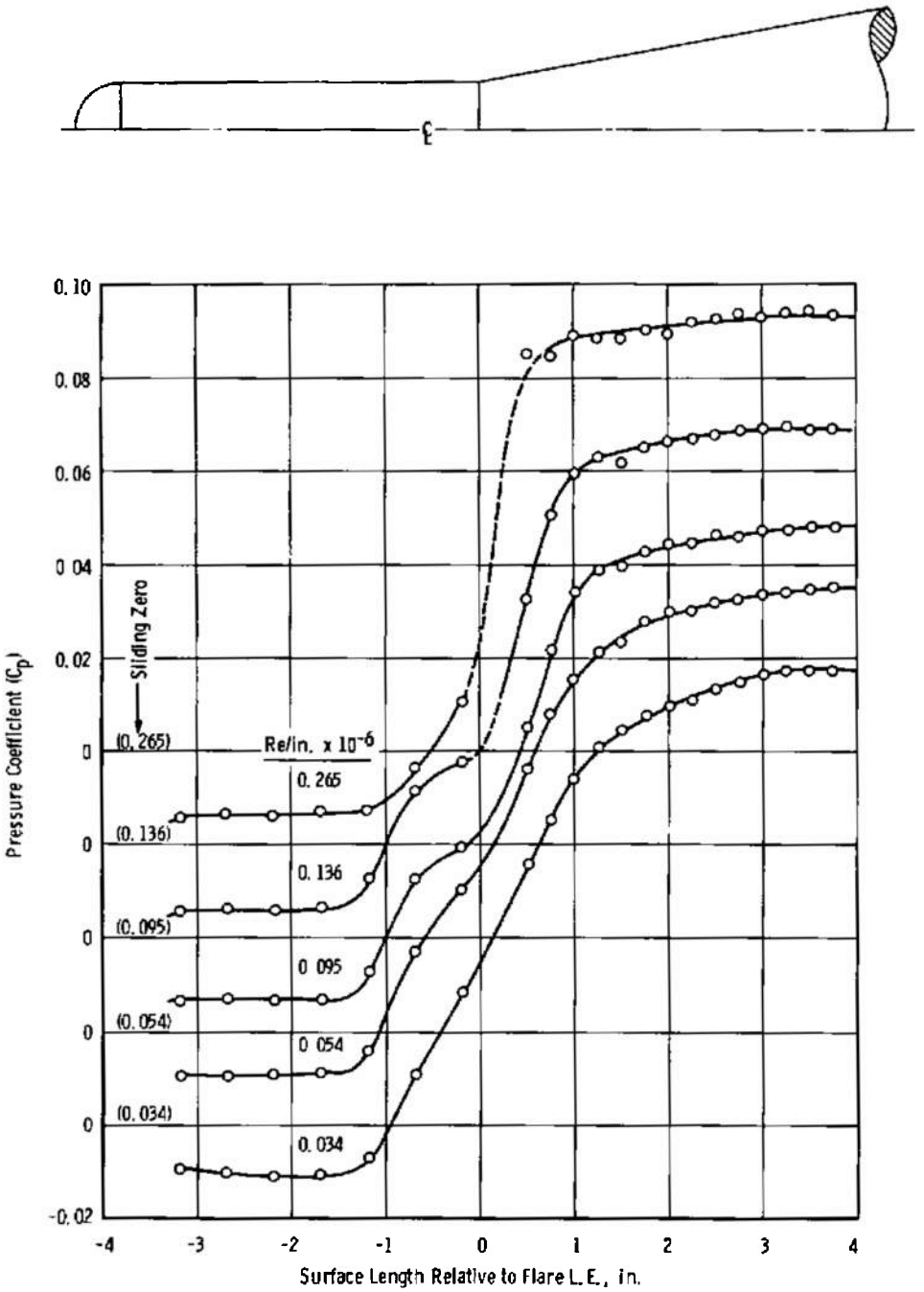

a. $M_\infty = 3$

Fig. 9 Pressure Distribution for Hemisphere Model, θ = 10 deg, Δx_c = 3.8 in.

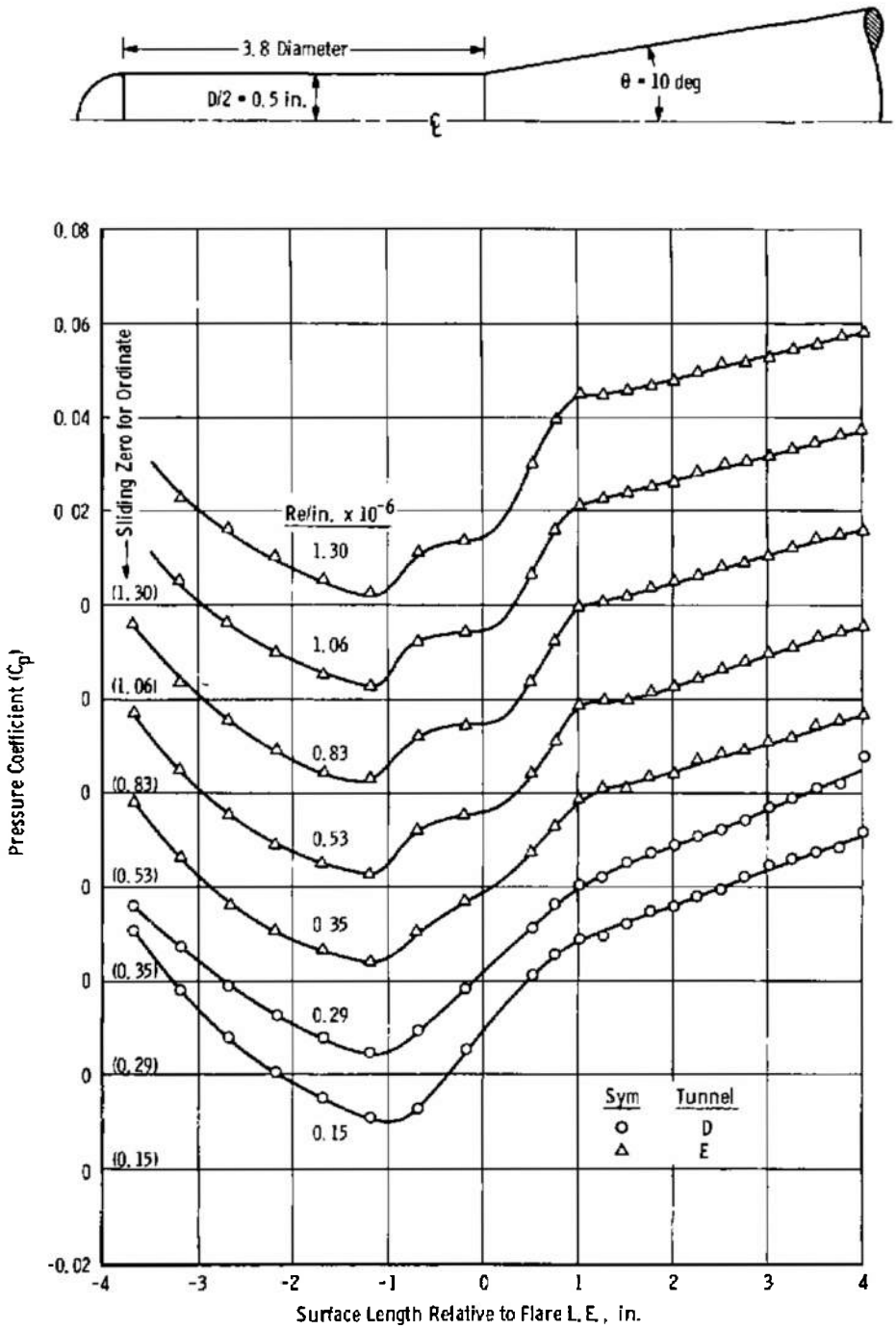

b. $M_\infty = 5$

Fig. 9 Continued

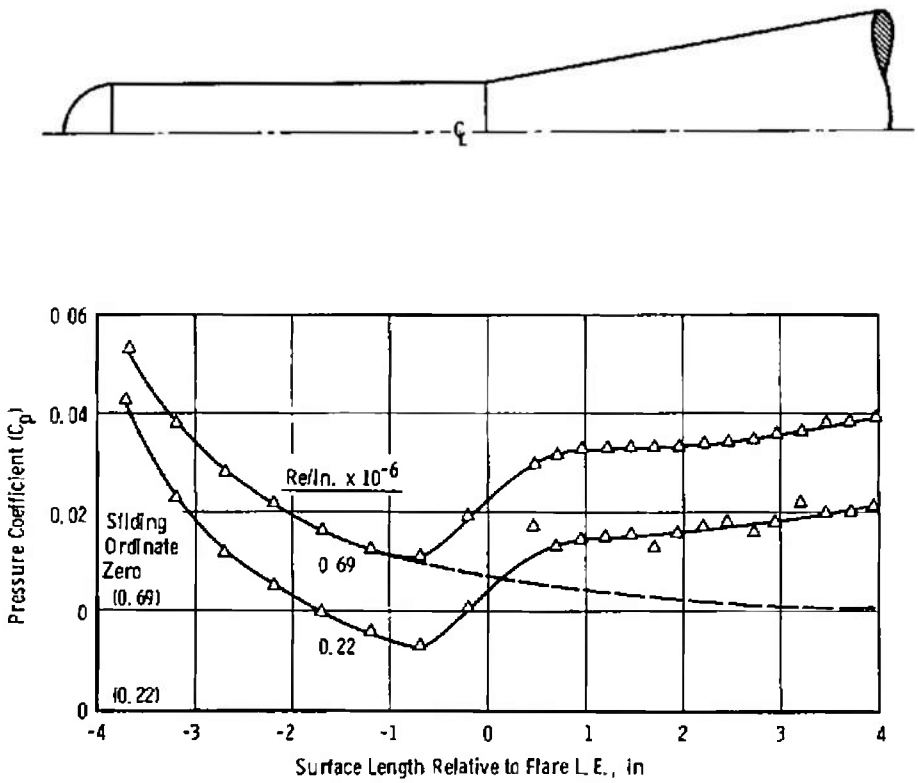

c. $M_\infty = 7$

Fig. 9 Concluded

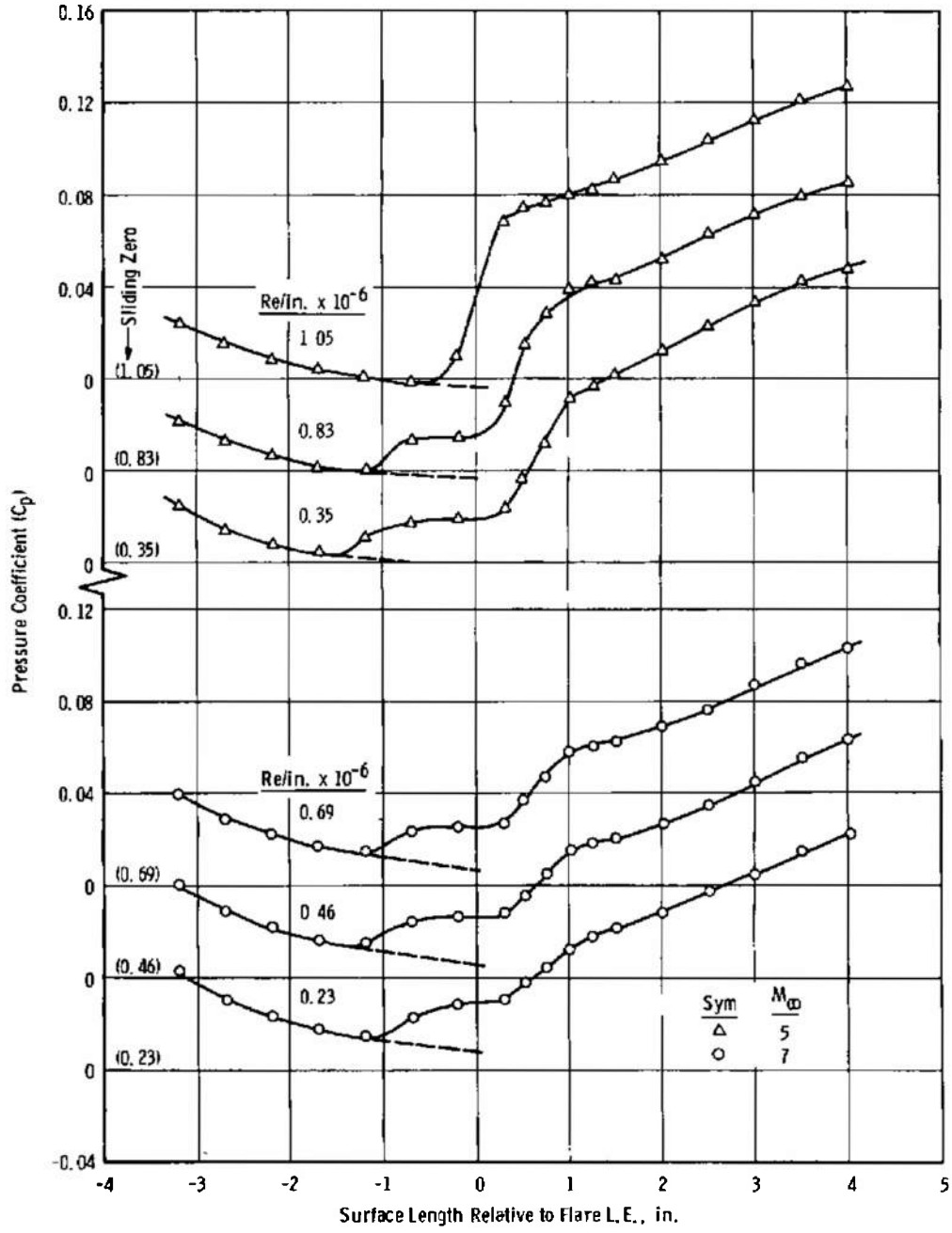

Fig. 10 Pressure Distribution for Hemisphere Model, θ = 15 deg, Δx_c = 3.8 in. at M_∞ = 5 and 7

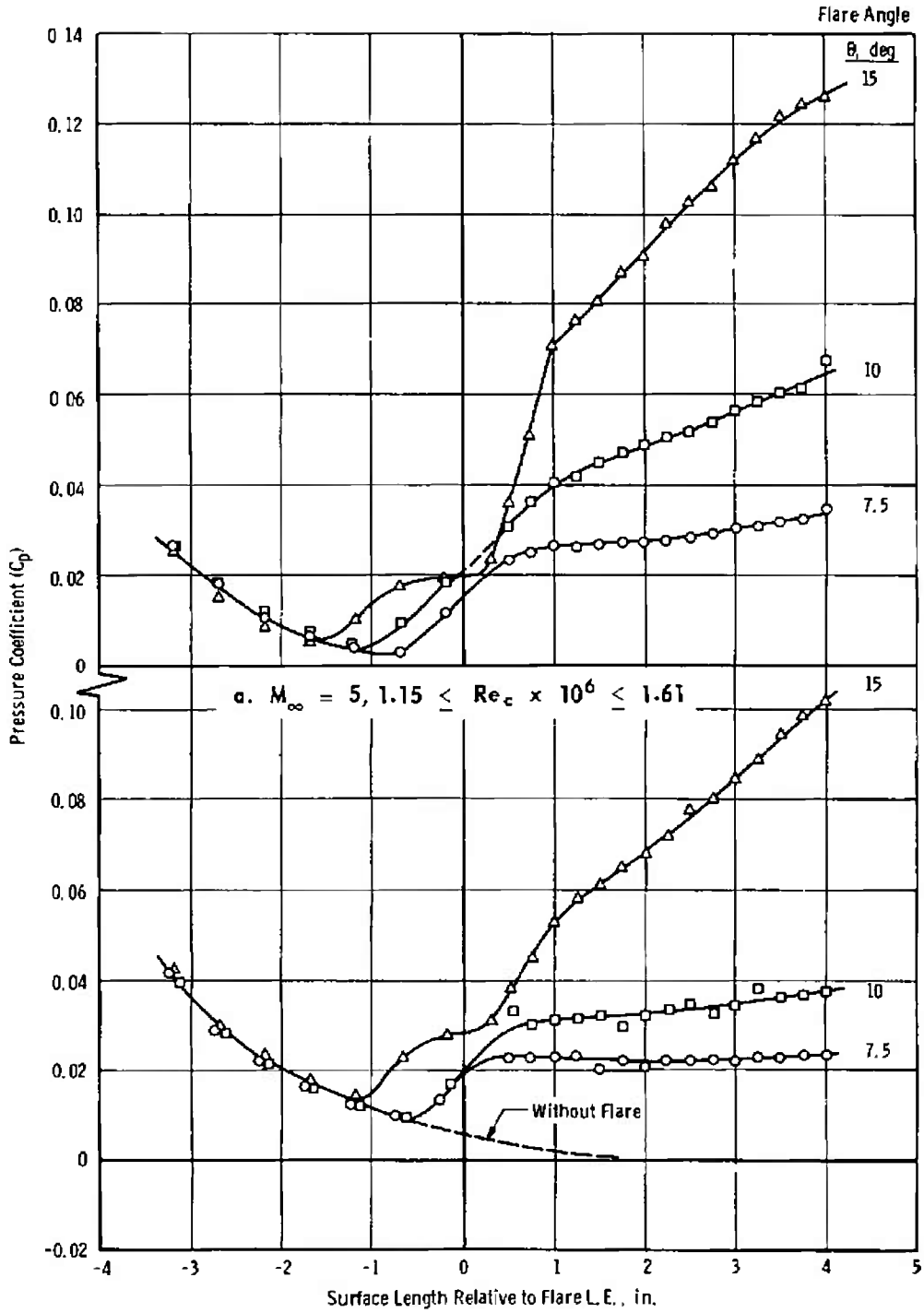

b. M_∞ = 7, Re_c = 1.01 x 10^6

Fig. 11 Effect of Flare Angle on Pressure Distribution for Hemisphere Model, Δx_c = 3.8 in.

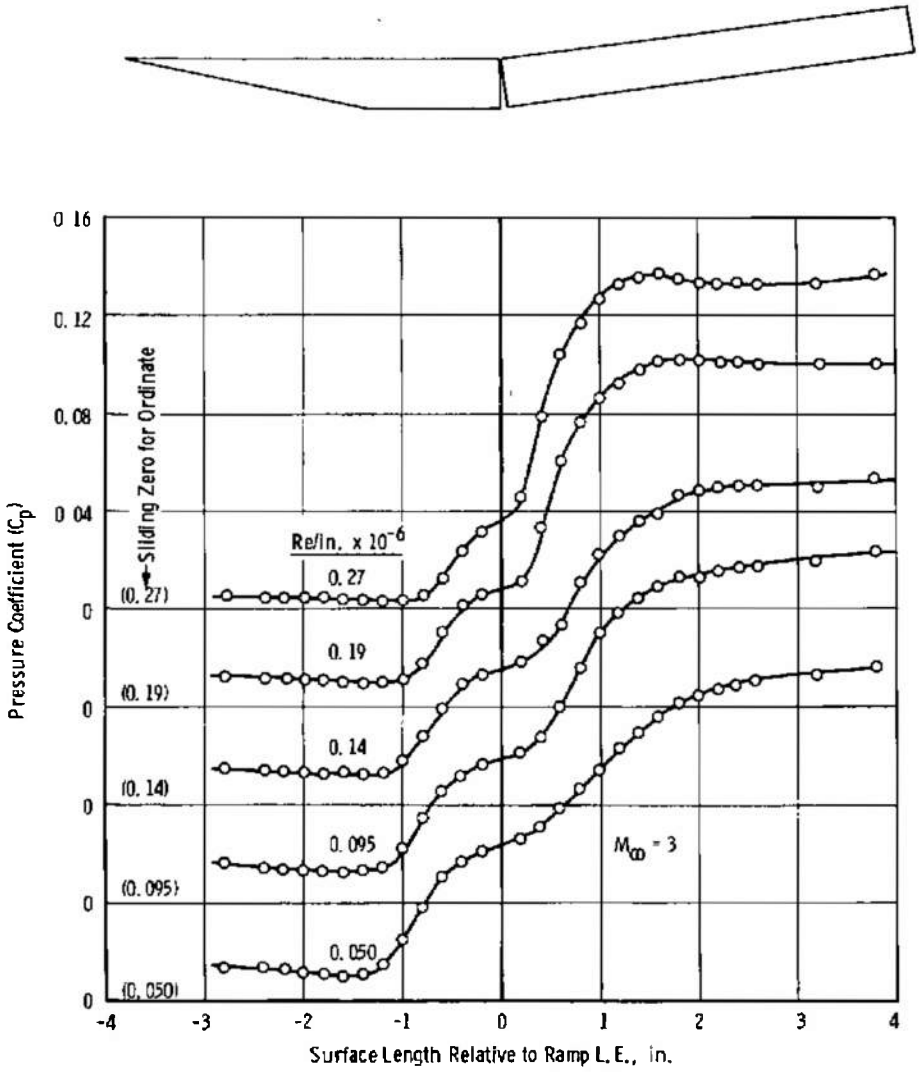

a. θ = 7.5 deg

Fig. 12 Pressure Distribution for Flat Plate Model, M_∞ = 3, x_c = 3.8 in.

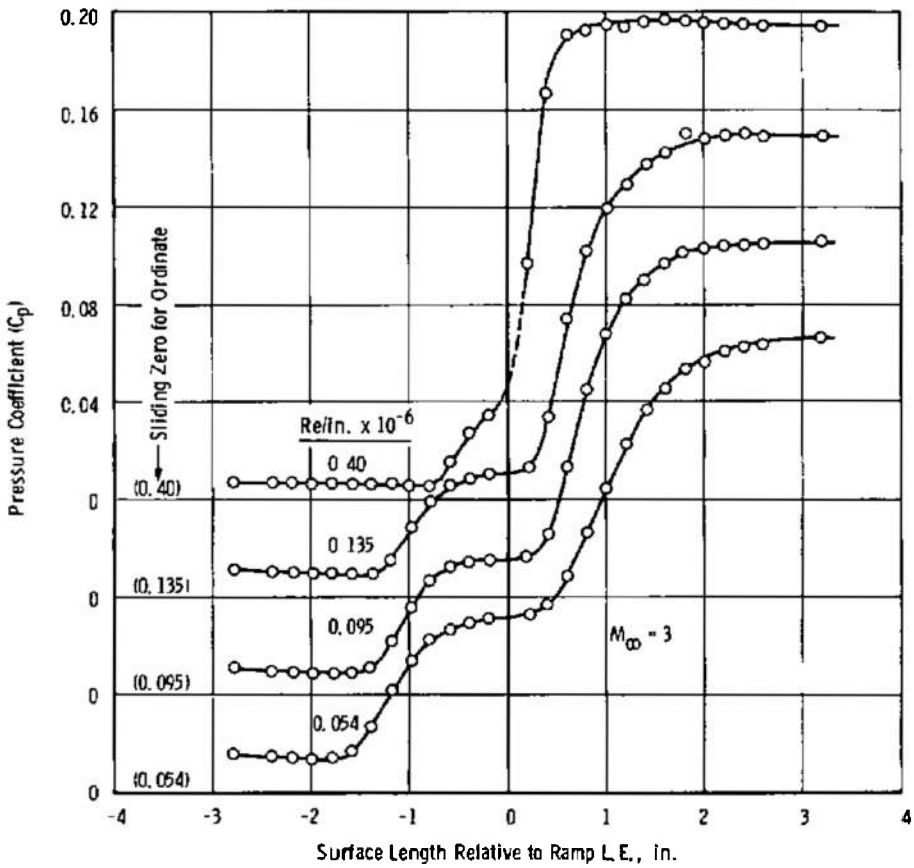

b. θ = 10 deg

Fig. 12 Continued

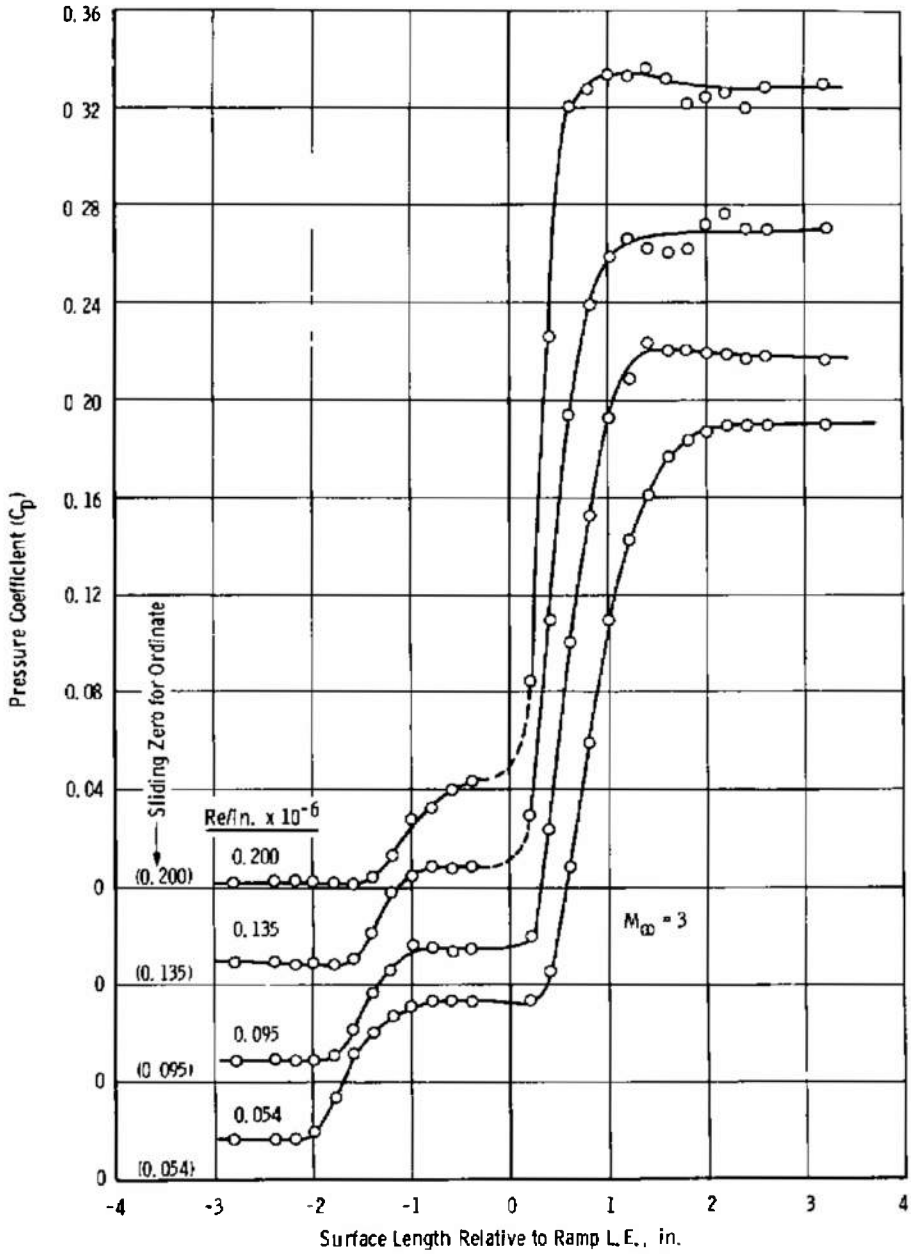

c. θ = 15 deg

Fig. 12 Concluded

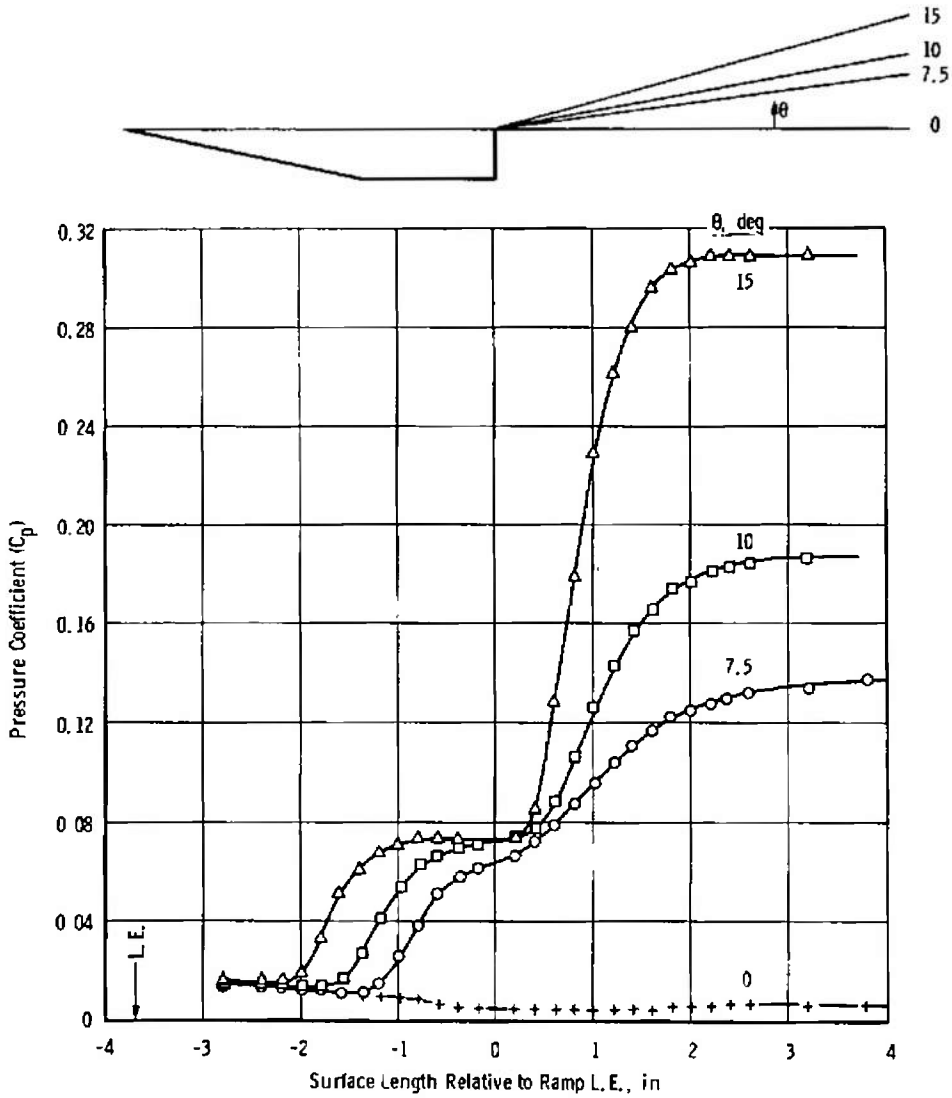

Fig. 13 Effect of Ramp Angle on Pressure Distribution for Flat Plate Model, $M_\infty = 3$, $x_c = 3.8$, $Re_c = 0.205 \times 10^6$

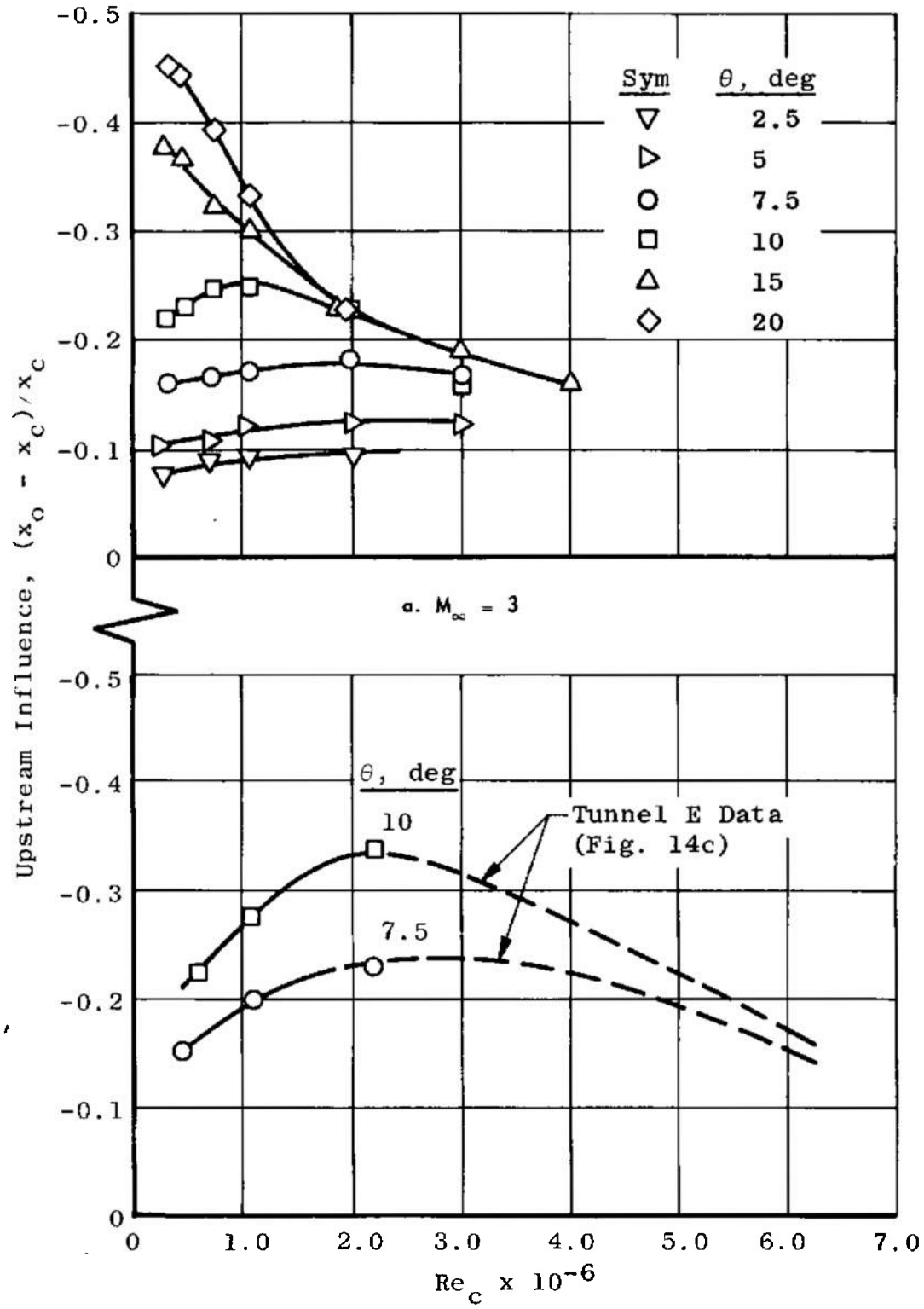

b. M_∞ = 5, Tunnel D

Fig. 14 Upstream Influence versus Reynolds Number for Sharp Cone Model, Δx_c = 3.8 in.

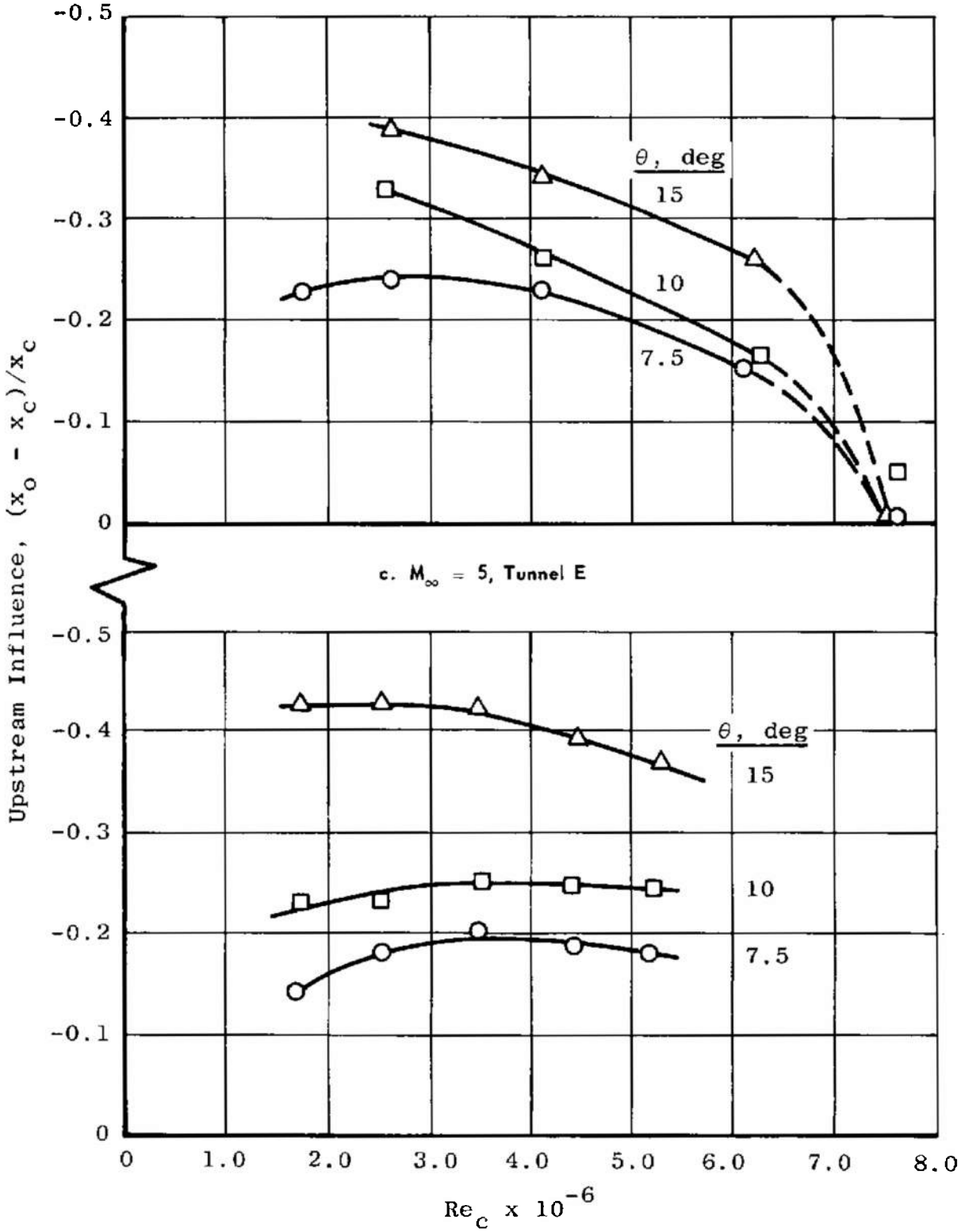

d. M_∞ = 7

Fig. 14 Concluded

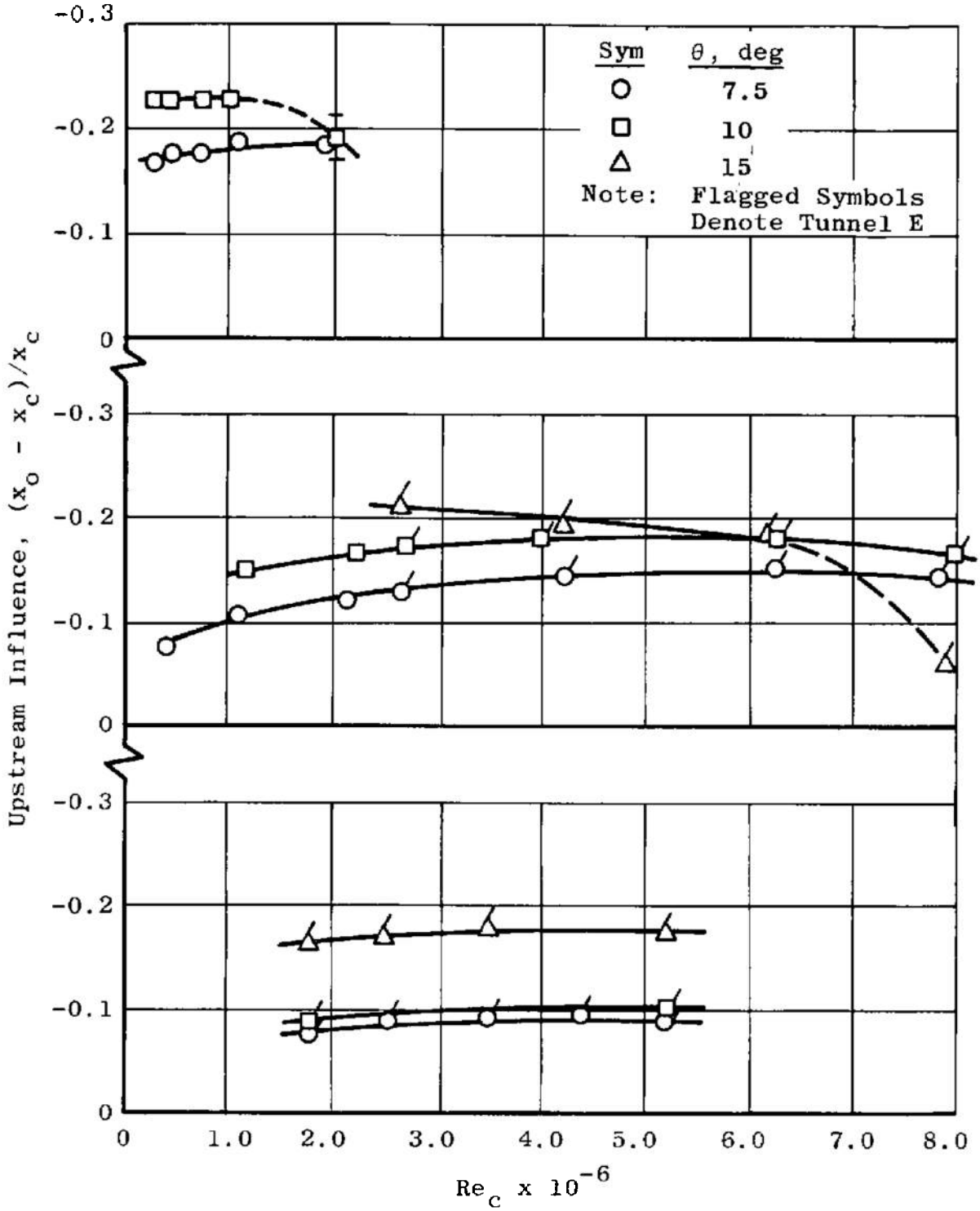

c. $M_\infty = 7$

Fig. 15 Upstream Influence versus Reynolds Number for Hemisphere Model, $\Delta x_c = 3.8$ in.

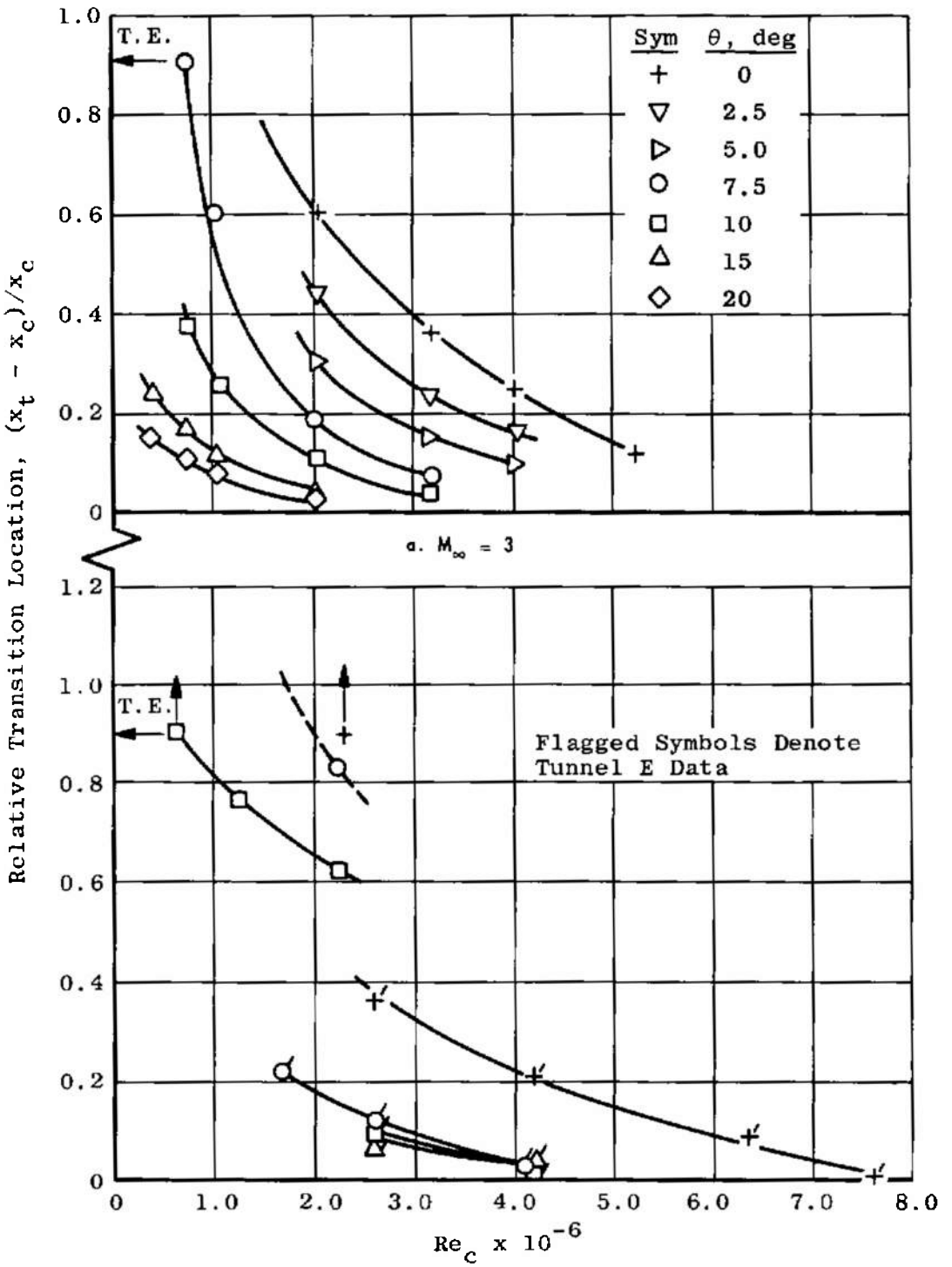

b. M_∞ = 5, Tunnels D and E

Fig. 16 Relative Transition Location versus Reynolds Number for Sharp Cone Model, Δx_c = 3.8 in.

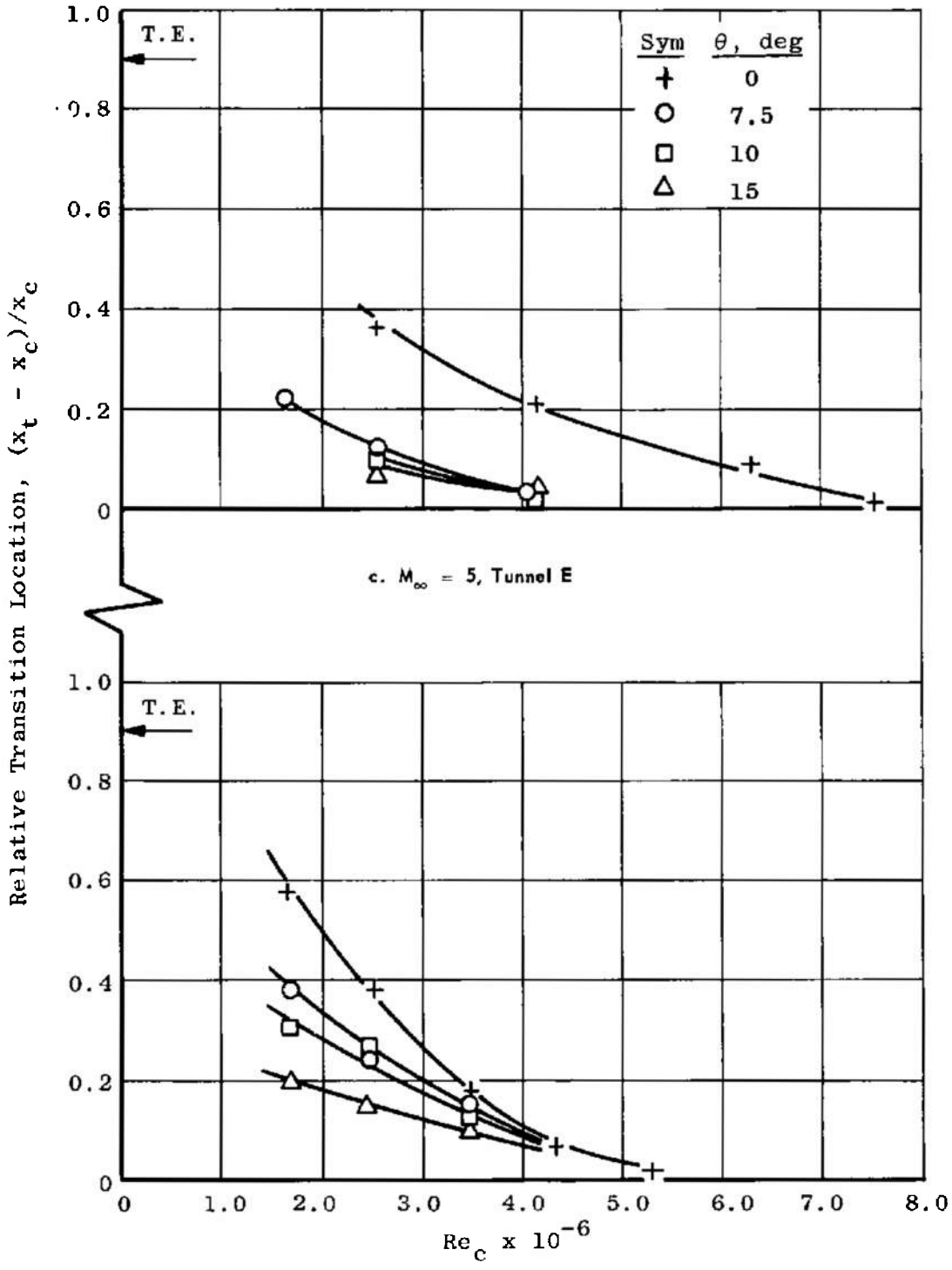

d. M_∞ = 7

Fig. 16 Concluded

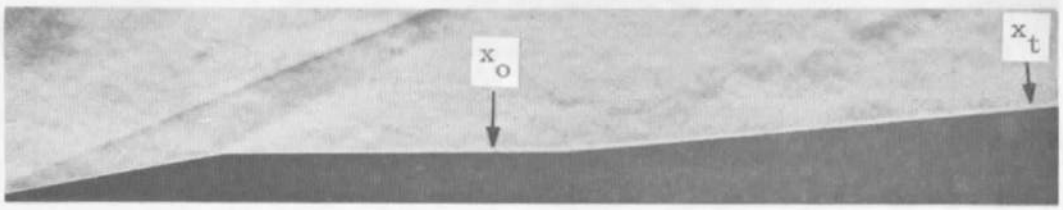

θ = 5 deg

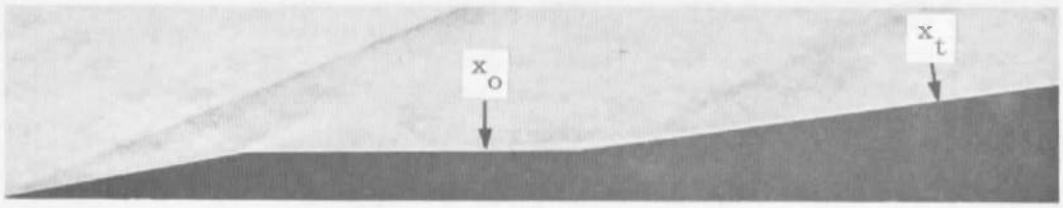

θ = 7.5 deg

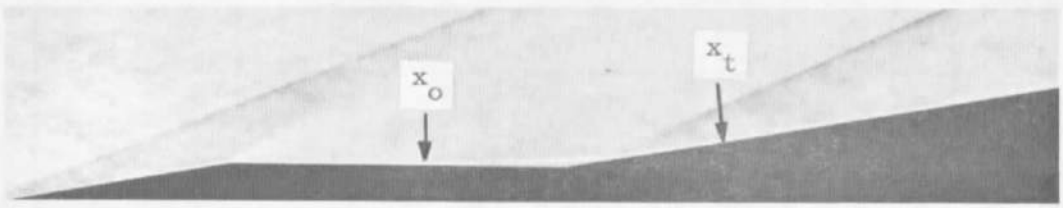

θ = 10 deg

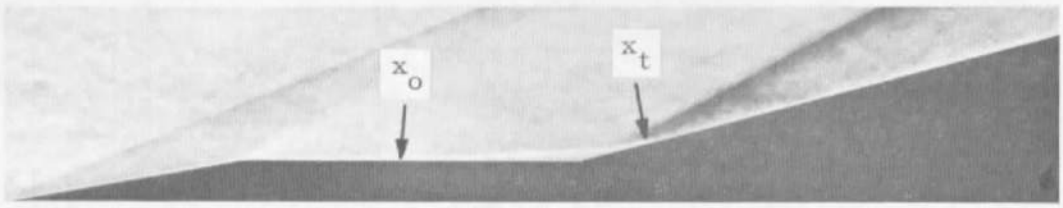

θ = 15 deg

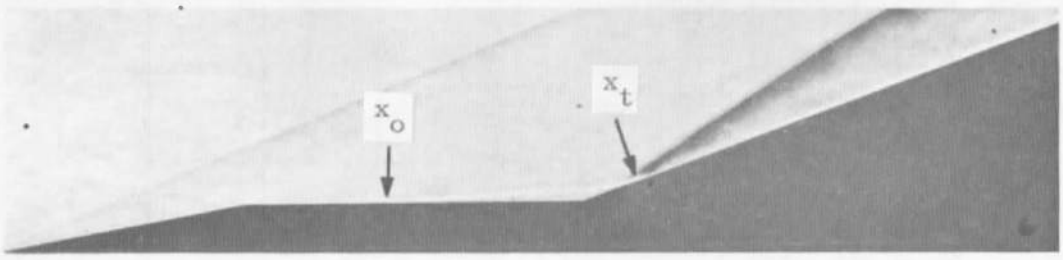

θ = 20 deg

Note: Tolerance on x_t Shown Equals 1 in.

a. θ = Variable, M_∞ = 3, Re_c = 0.90 x 10^6

Fig. 17 Schlieren Pictures of Sharp Cone Models, Δx_c = 3.8 in.

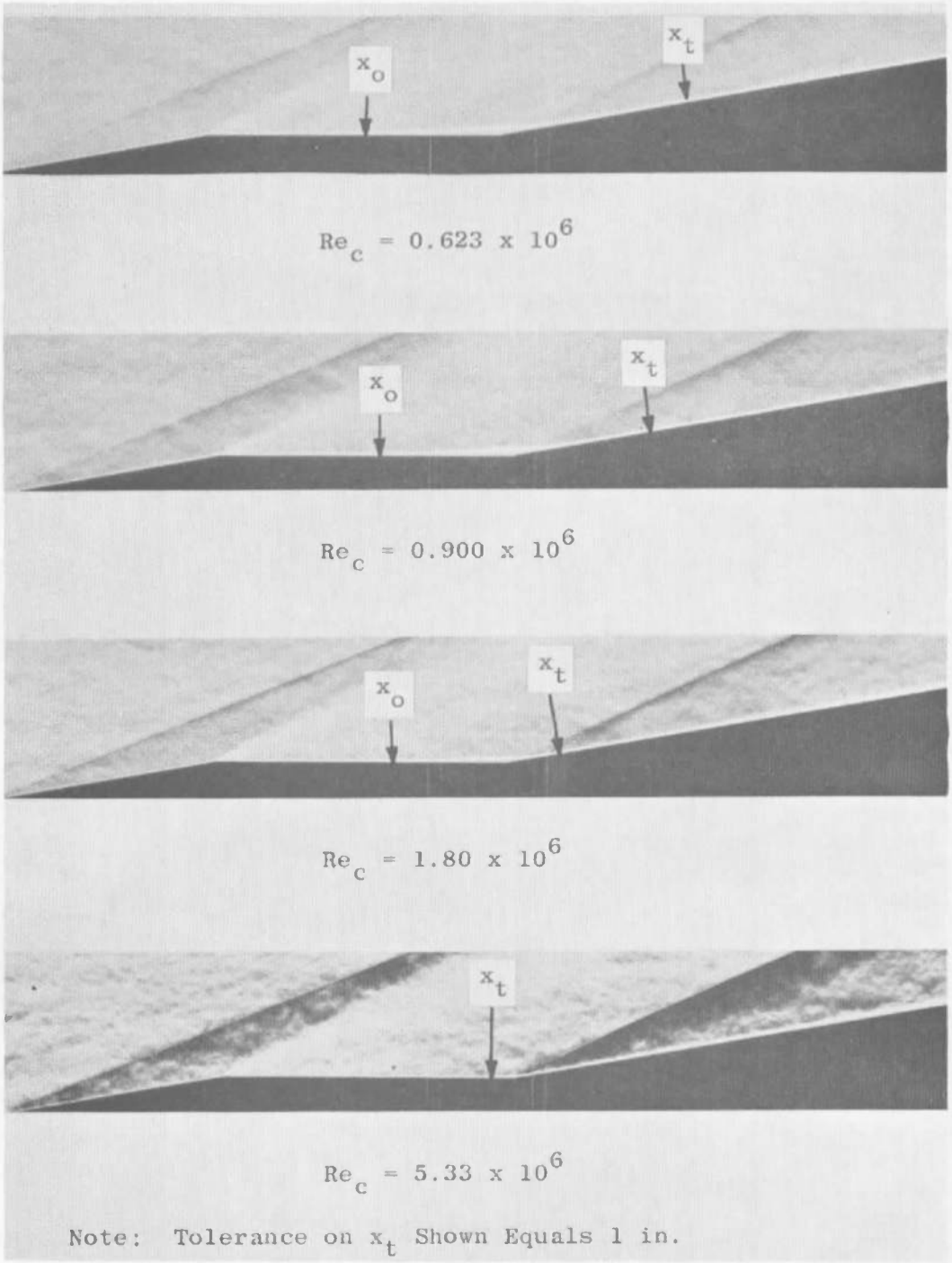

b. θ = 10 deg, M_∞ = 3, Re_c = Variable

Fig. 17 Continued

$Re_c = 0.48 \times 10^6$

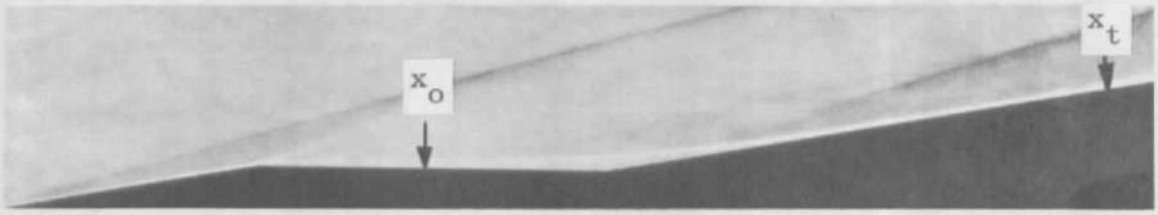

$Re_c = 1.00 \times 10^6$

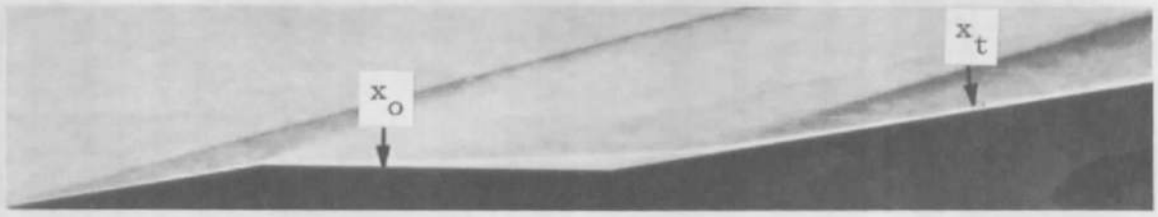

$Re_c = 1.93 \times 10^6$

Note: Tolerance on x_t Shown Equals 1 in.

c. θ = 10 deg, M_∞ = 5, Re_c = Variable

Fig. 17 Concluded

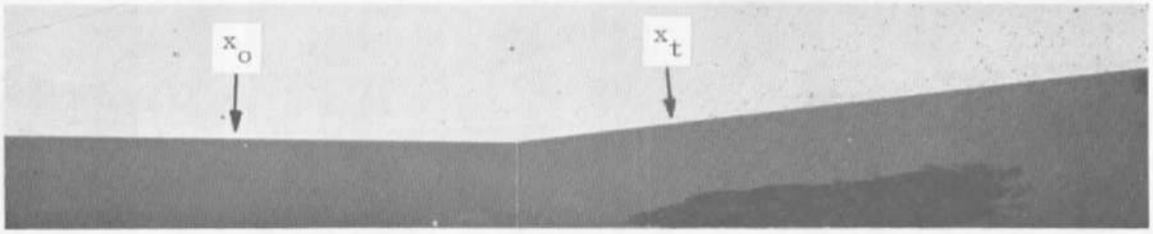

$Re_c = 2.33 \times 10^6$

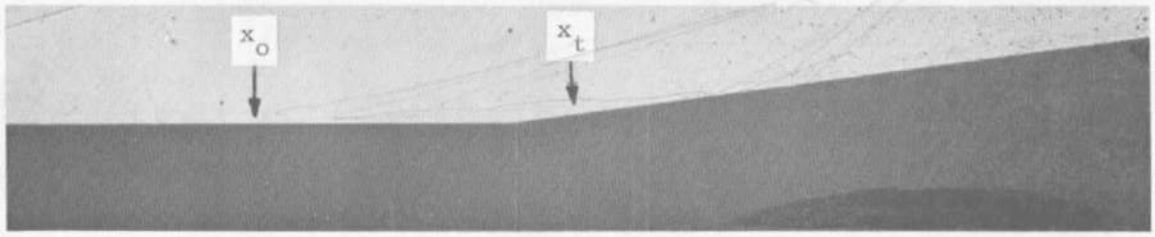

$Re_c = 3.67 \times 10^6$

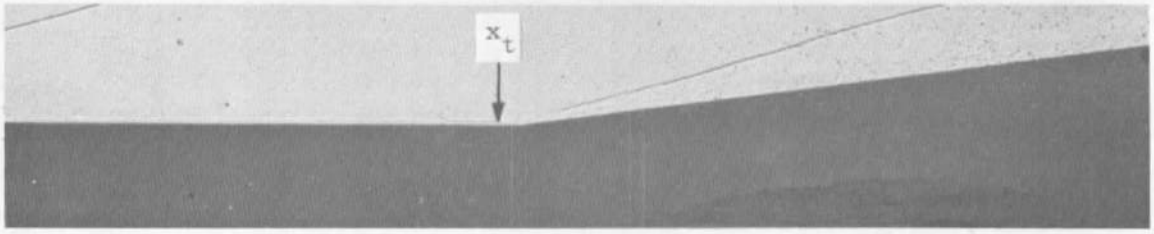

$Re_c = 6.80 \times 10^6$

Note: Tolerance on x_t Shown Equals 1 in.

Fig. 18 Shadowgraph Pictures of Sharp Cone Model, Δx_c = 3.8 in., θ = 7.5 deg, M_∞ = 5, Re_c = Variable

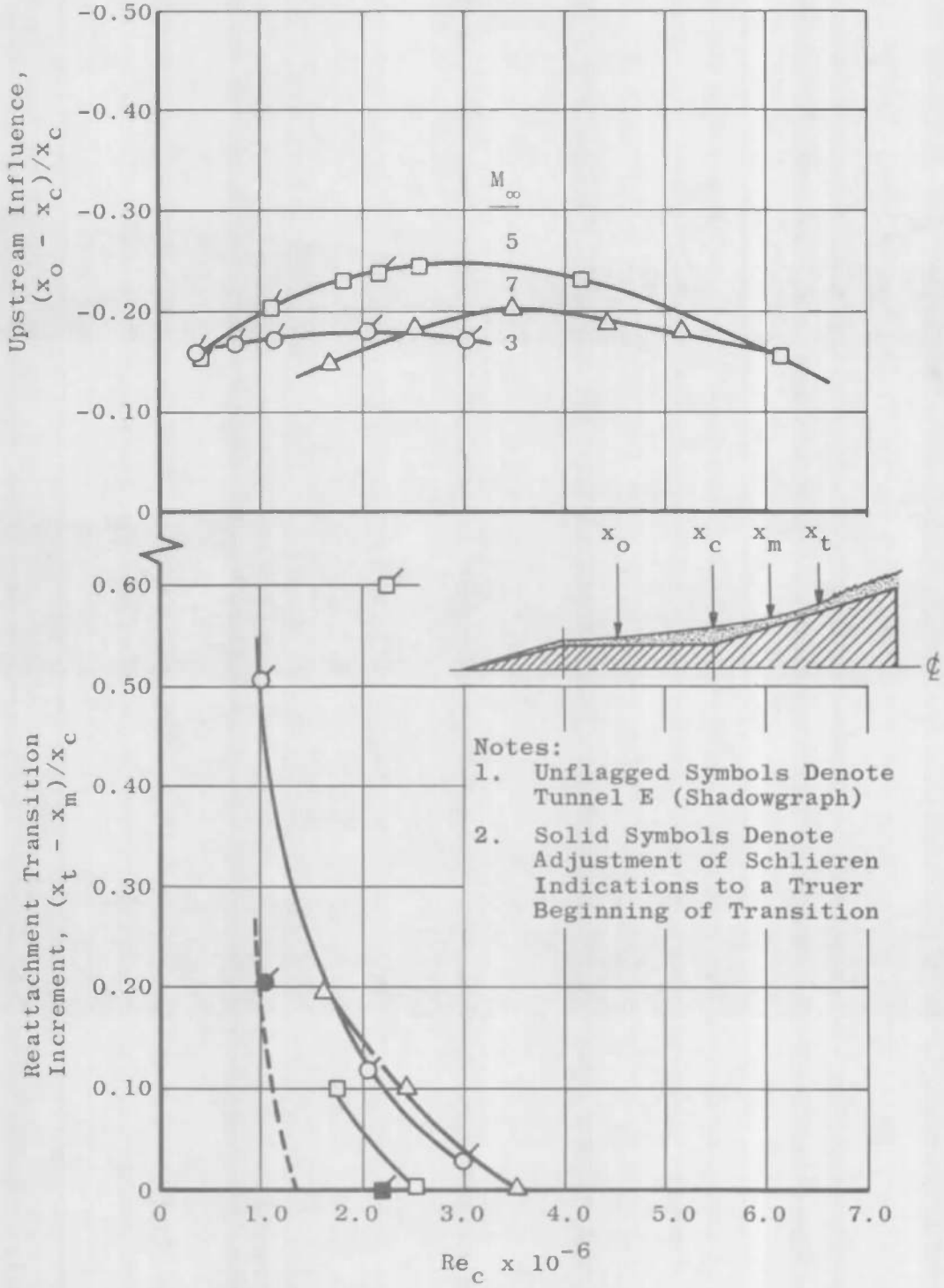

a. θ = 7.5 deg

Fig. 19 Correlation of Reattachment Transition Increment with Upstream Influence for Sharp Cone Models

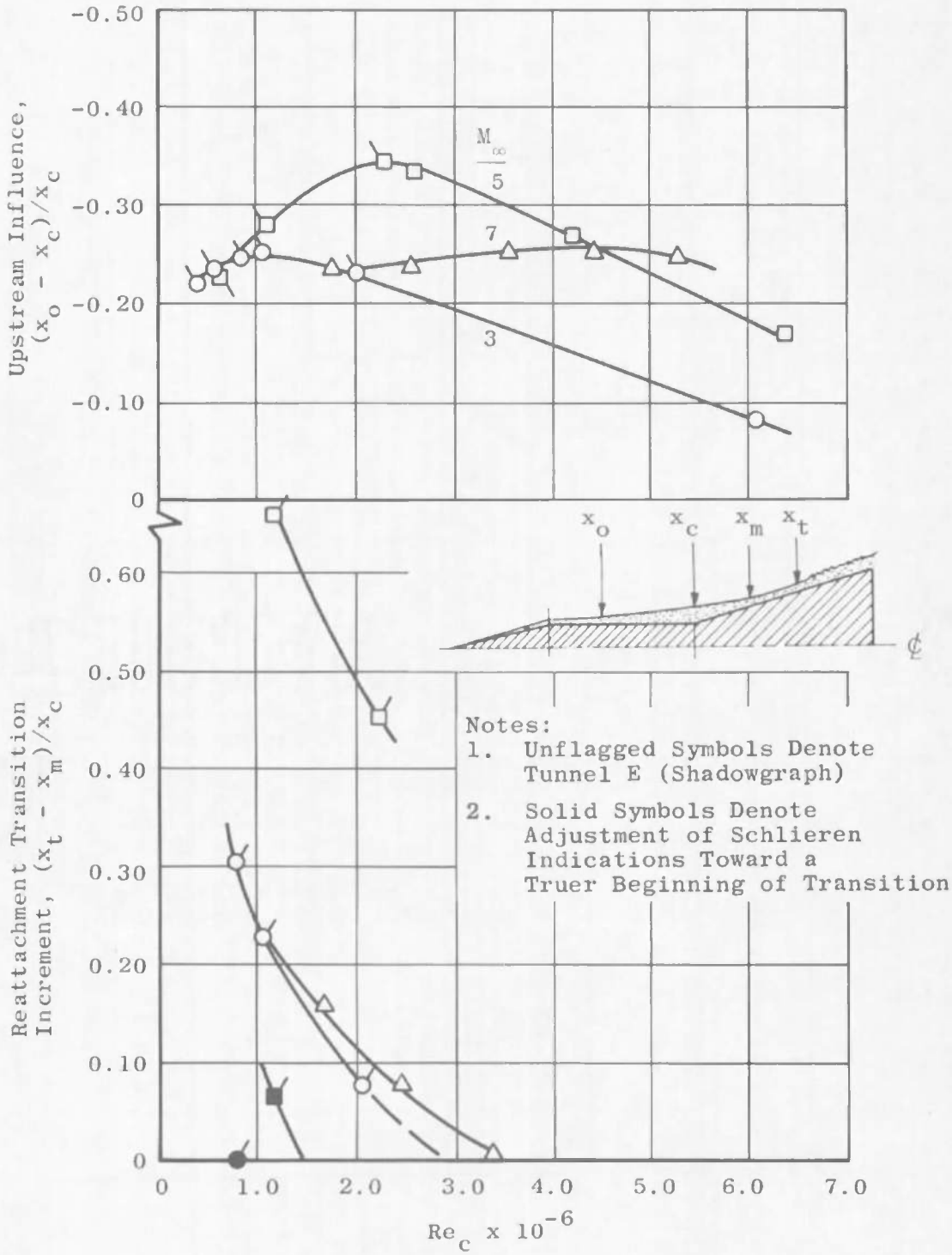

b. θ = 10 deg

Fig. 19 Continued

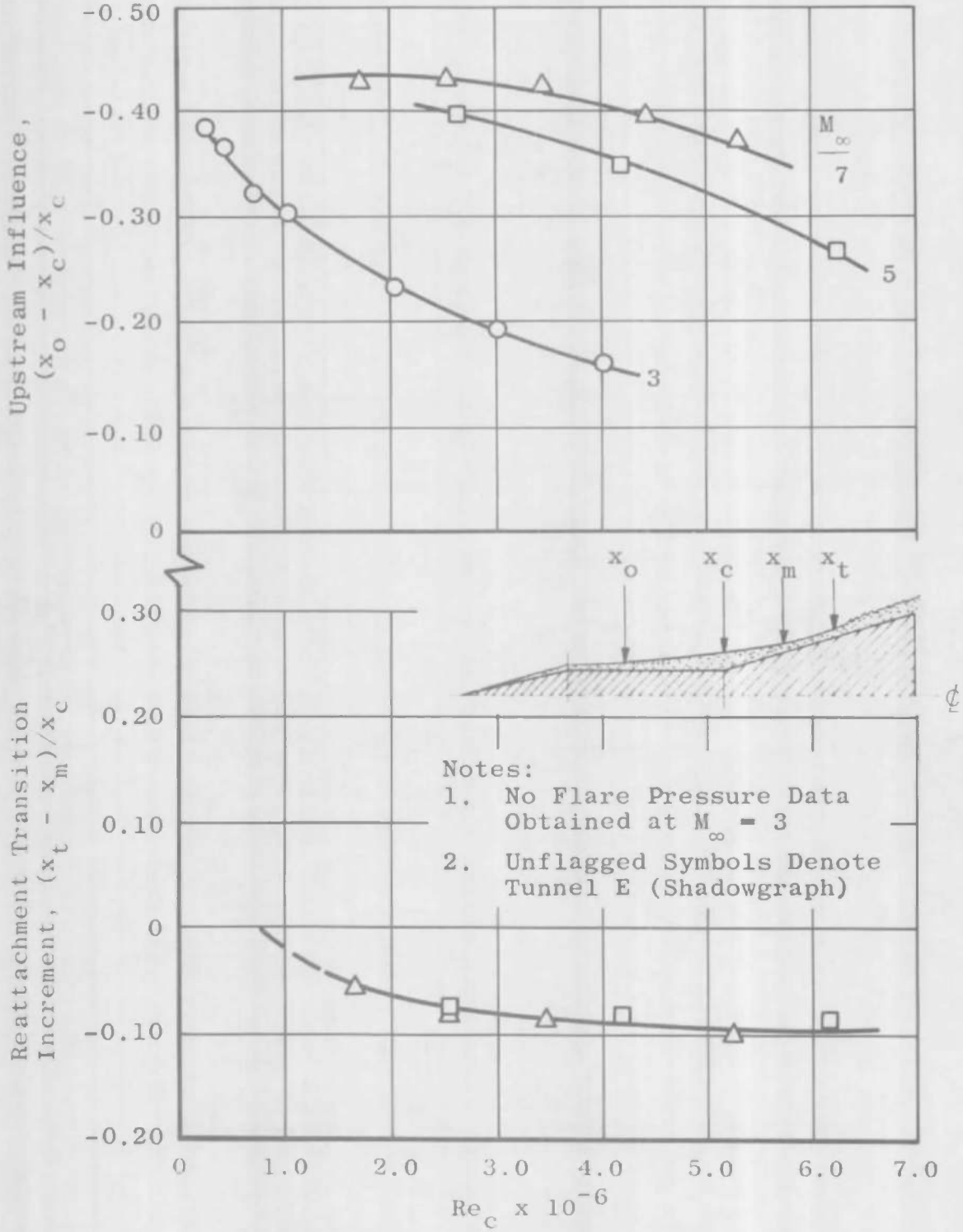

c. θ = 15 deg

Fig. 19 Concluded

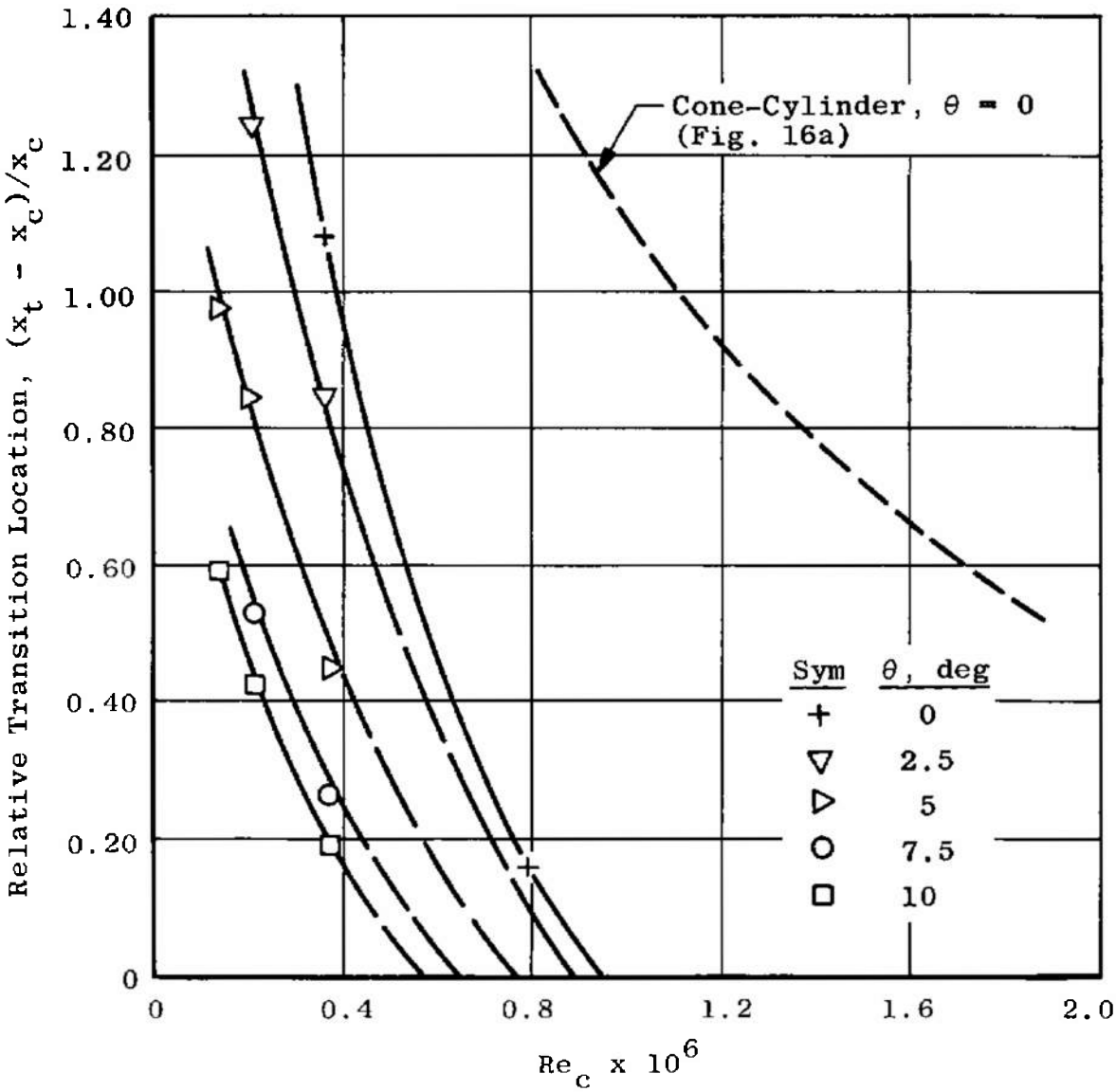

Fig. 20 Relative Transition Location versus Reynolds Number for Flat Plate Model, x_c = 3.8 in., M_∞ = 3

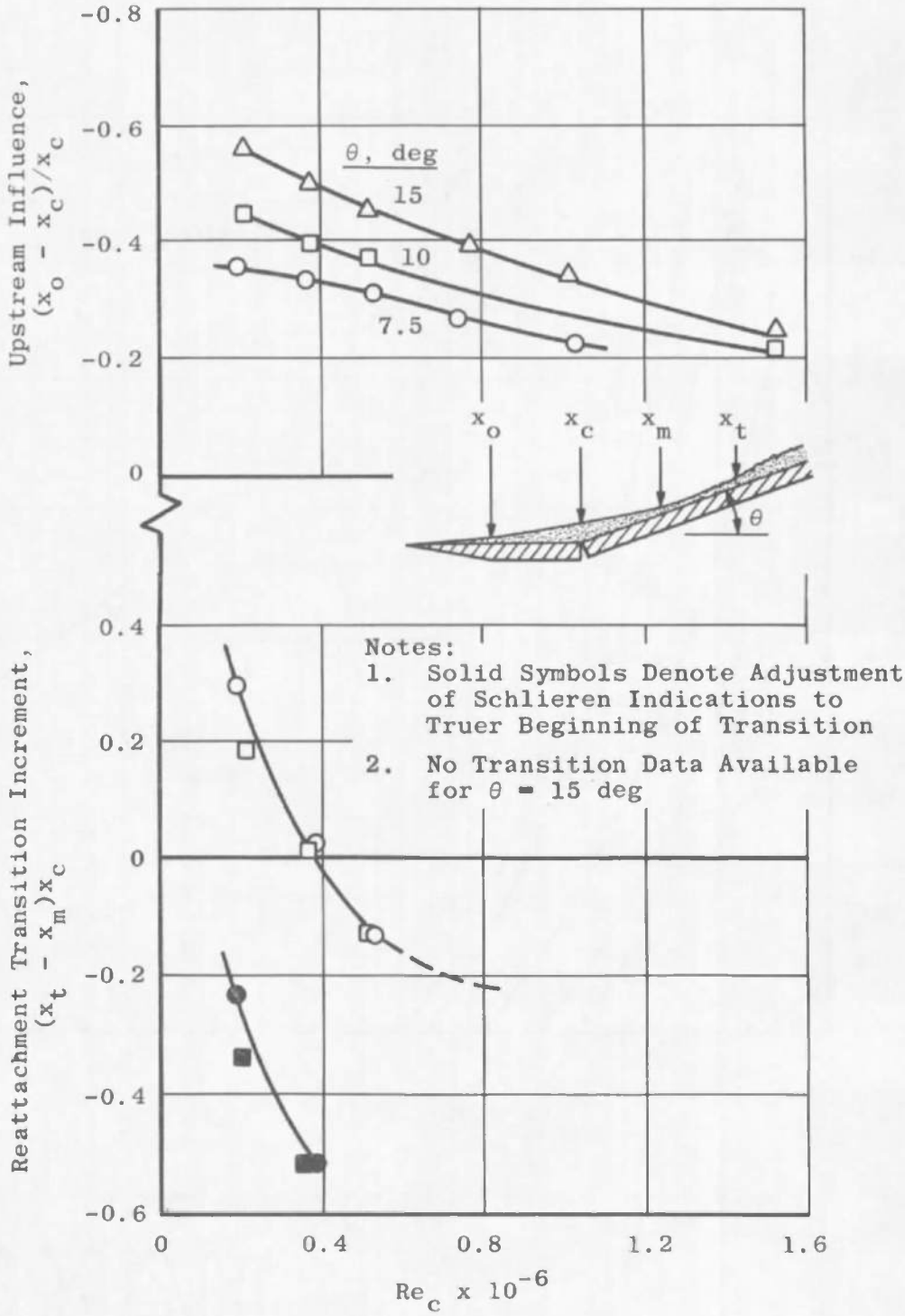

Fig. 21 Correlation of Reattachment Transition Increment with Upstream Influence for Flat Plate Model, x_c = 3.8 in., M_∞ = 3

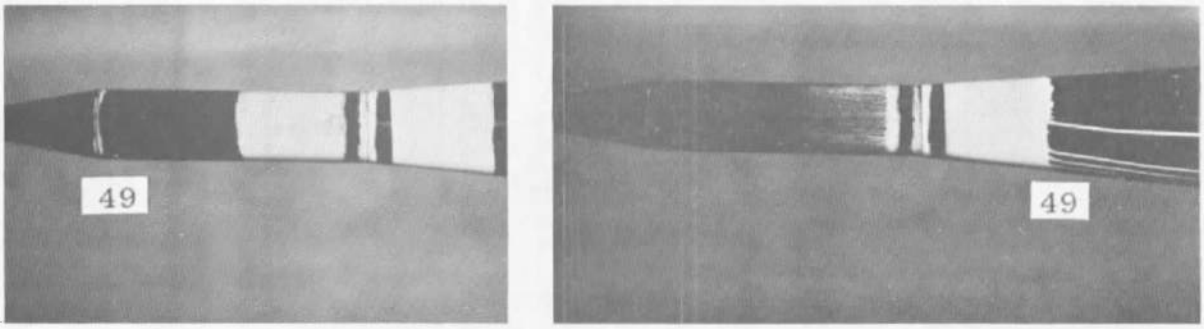

a. θ = 5 deg

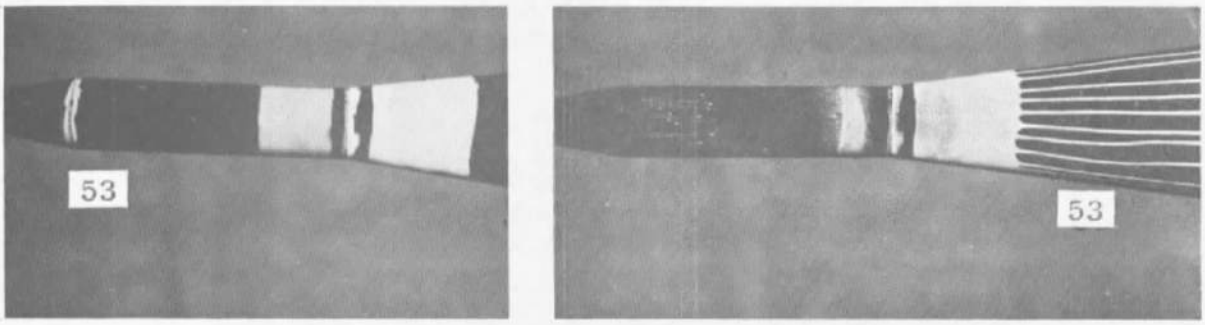

b. θ = 7.5 deg

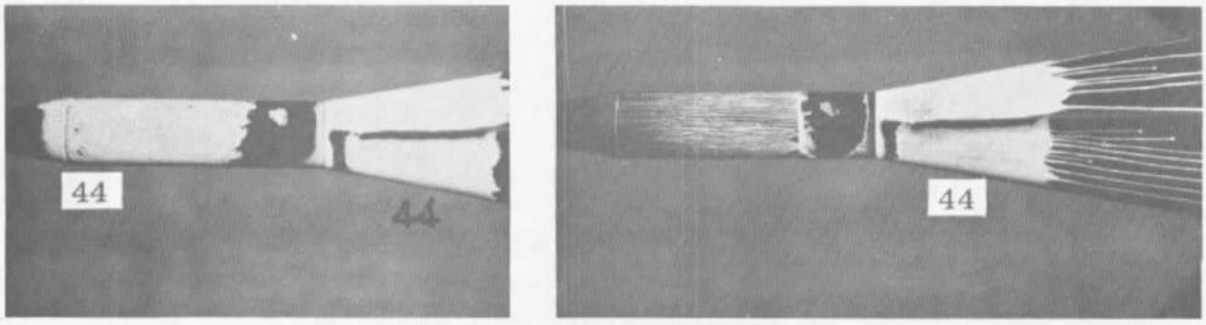

c. θ = 10 deg

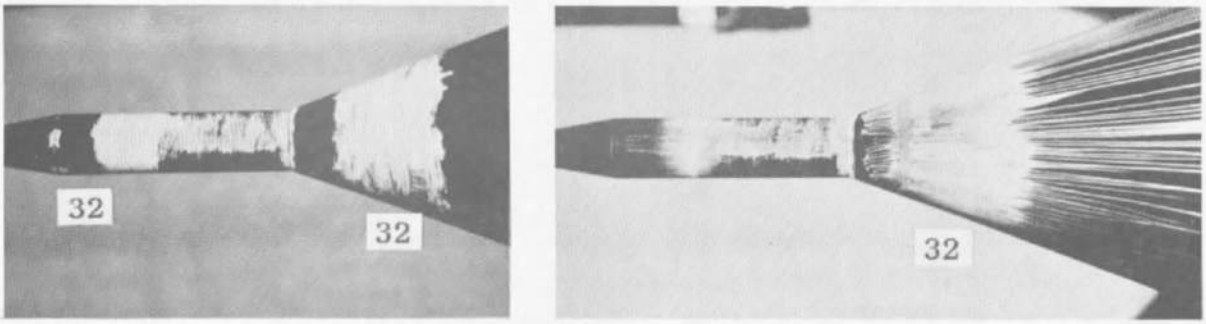

d. θ = 20 deg

Fig. 22 Typical Oil Film Data for Sharp Cone Model, Δx_c = 3.8 in., M_∞ = 3, Re_c = 0.36 x 10^6

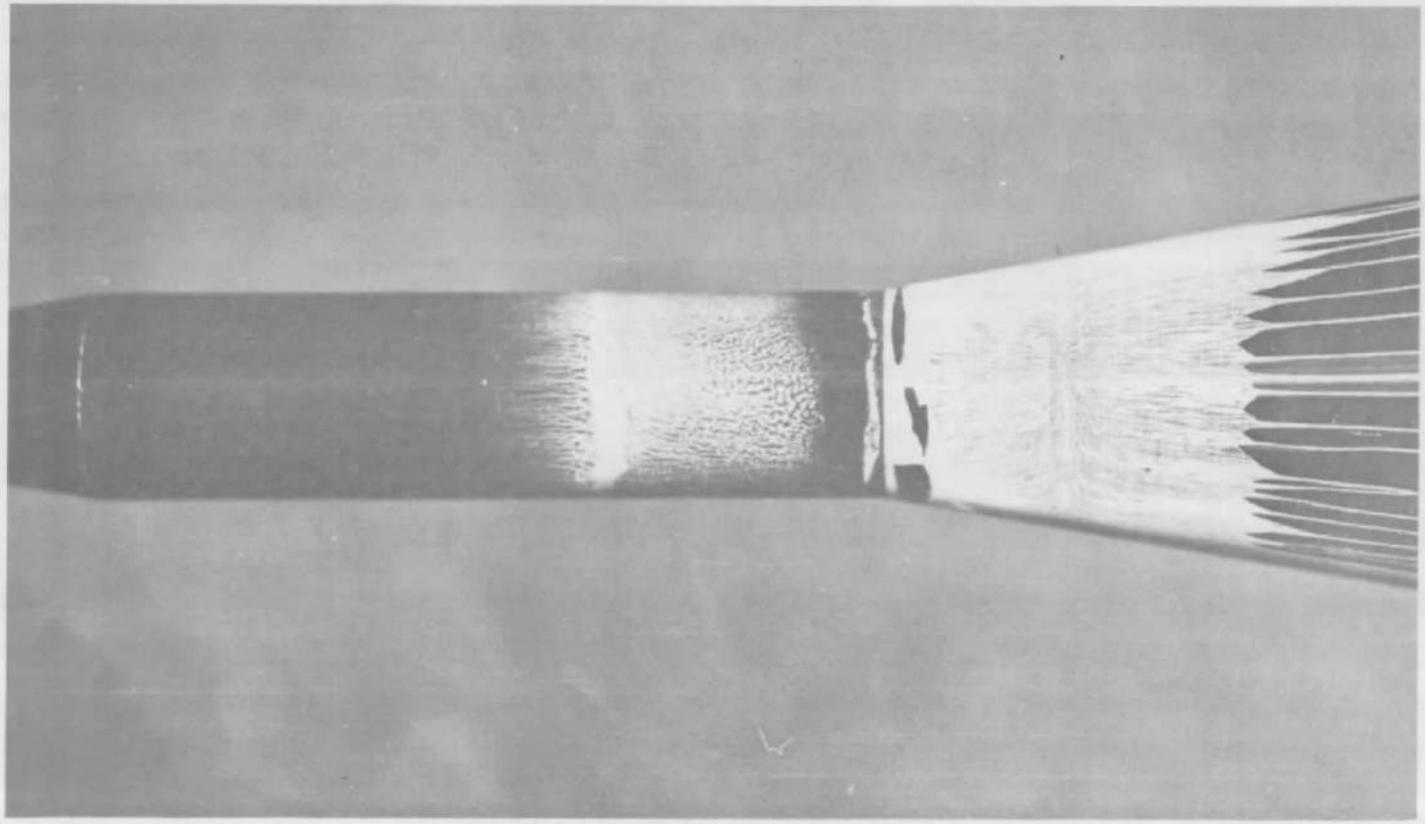

Fig. 23 Enlargement of Oil Film Picture for Sharp Cone Model, $\Delta x_c = 3.8$ in., $M_\infty = 3$, $Re_c = 0.90 \times 10^6$, $\theta = 10$ deg

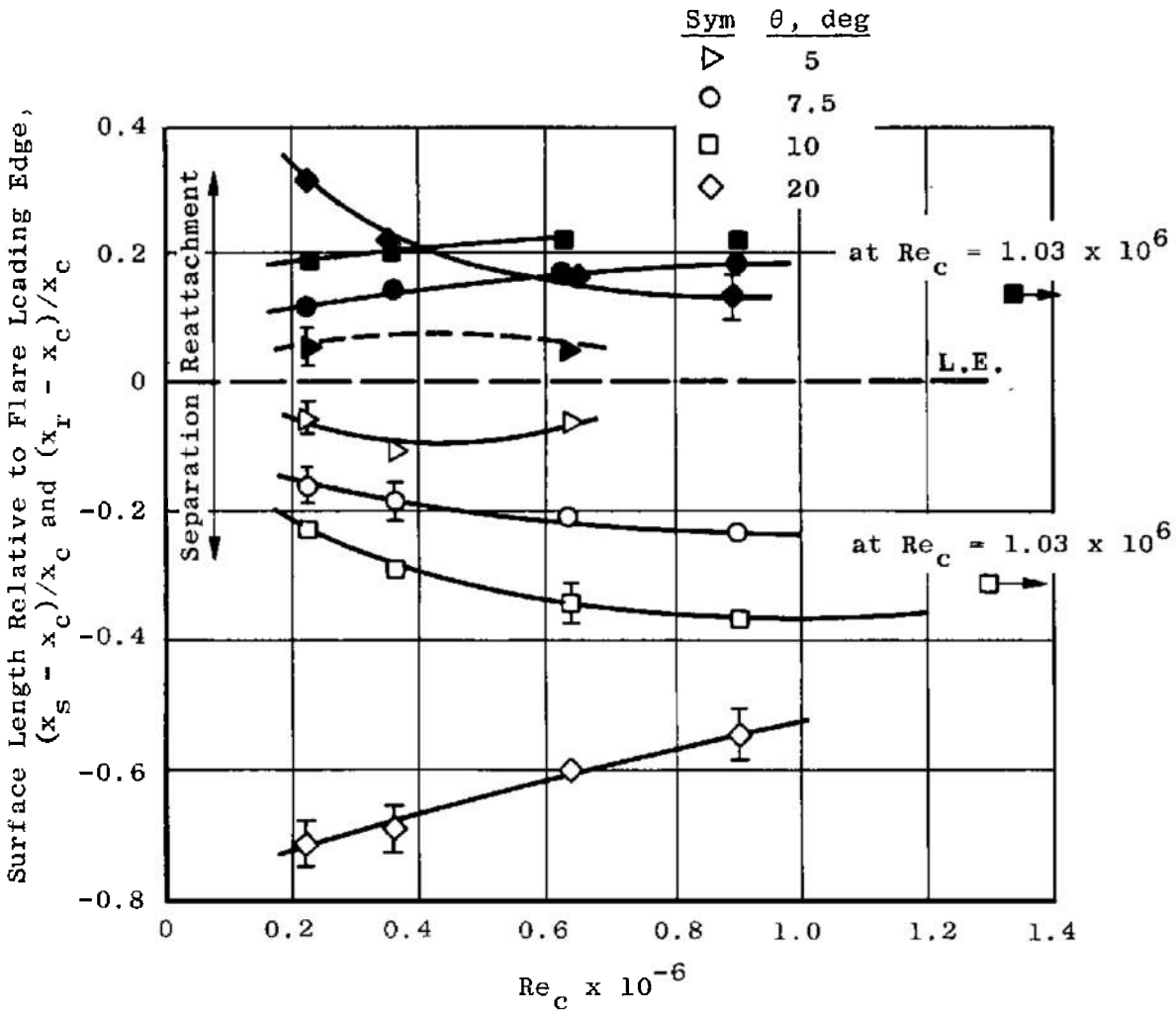

Fig. 24 Variation of Separation and Reattachment Locations with Reynolds Number at M_∞ = 3 on Sharp Cone Model, Δx_c = 3.8 in.

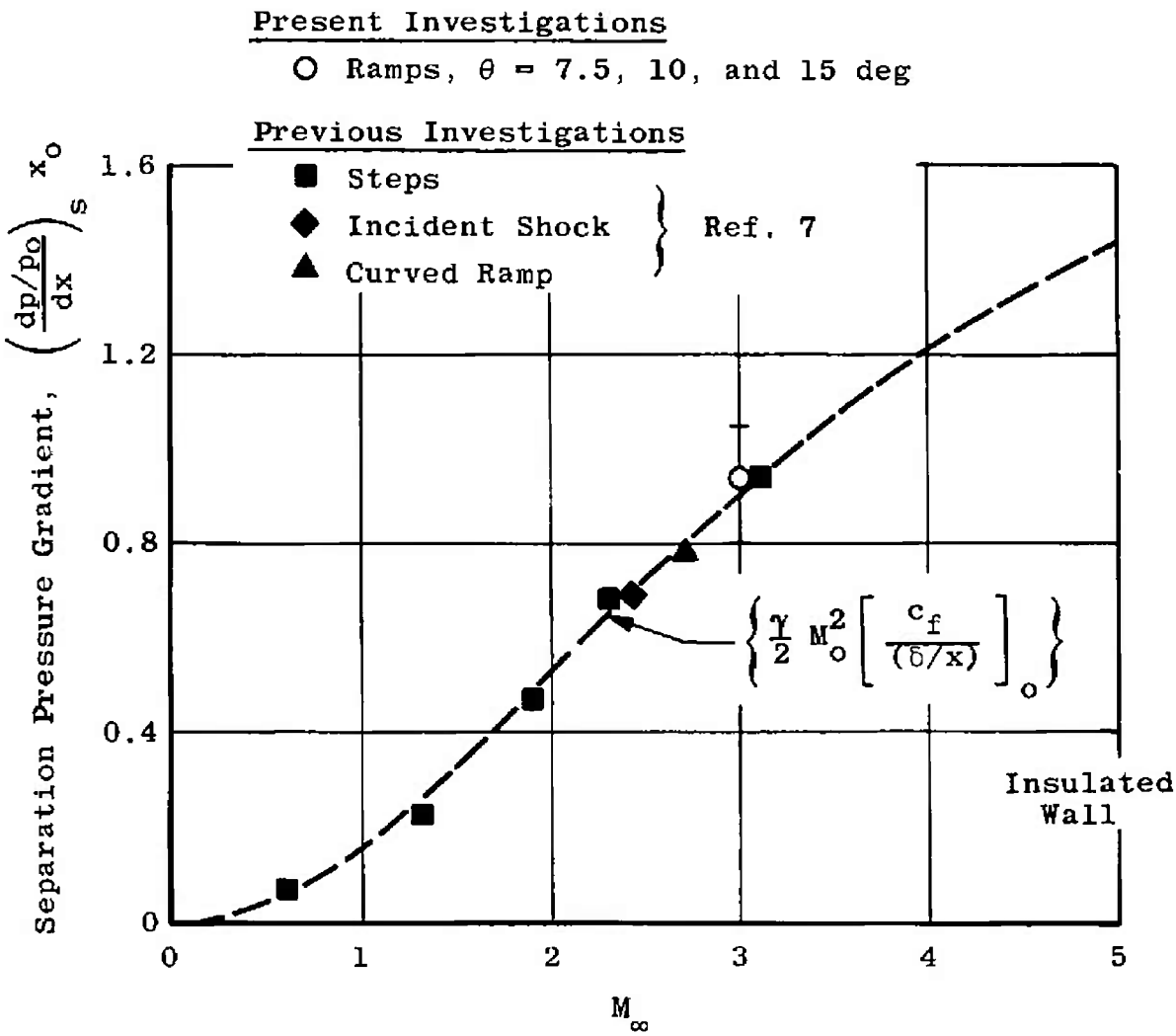

Fig. 25 Separation Pressure Gradient versus Mach Number, Adiabatic Wall Data

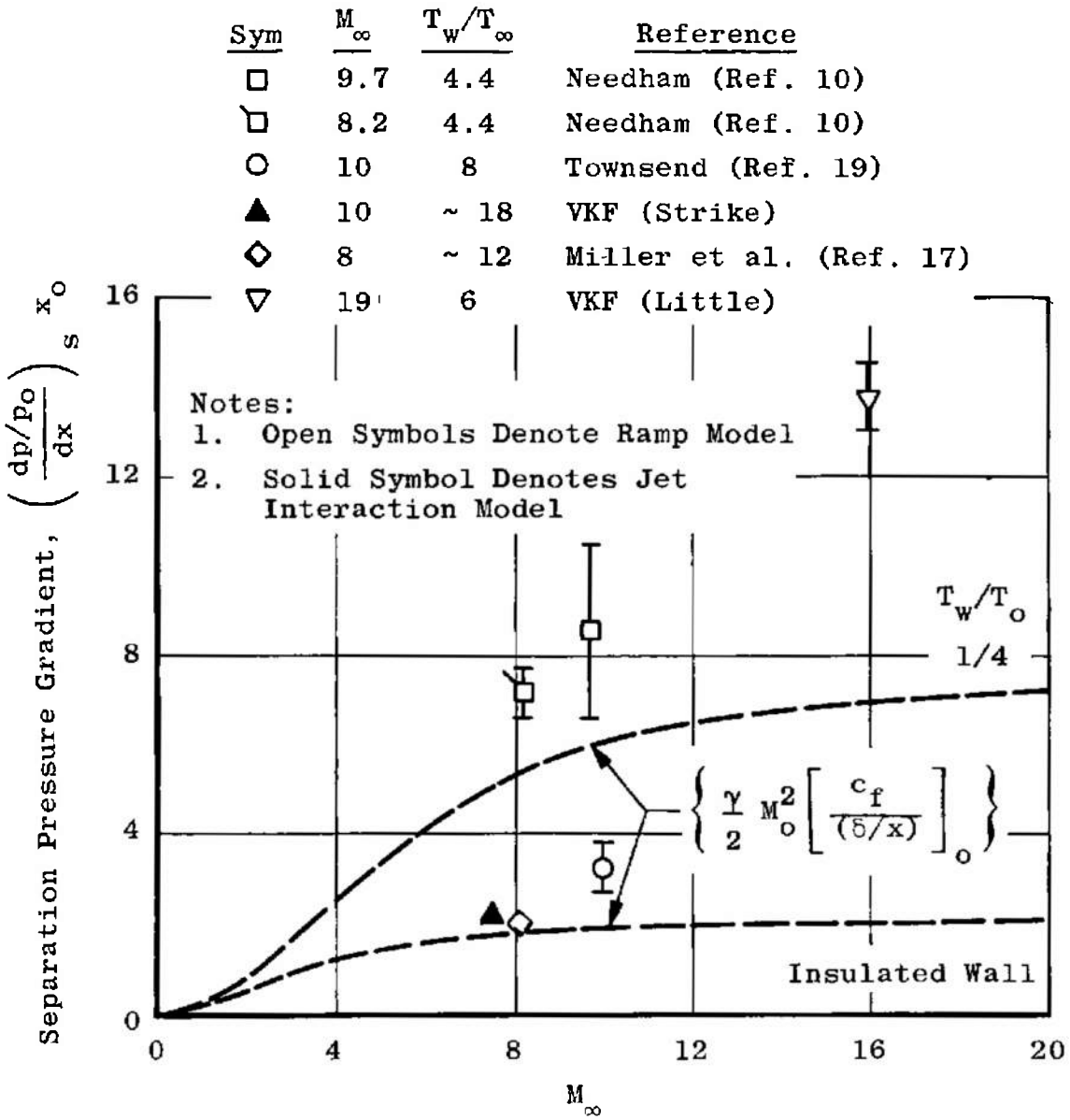

Fig. 26 Separation Pressure Gradient versus Mach Number, Cold Wall Data

Security Classification

DOCUMENT CONTROL DATA - R&D

(Security classification of title body of abstract and indexing annotation must be entered when the overall report is classified)

1 ORIGINATING ACTIVITY *(Corporate author)* Arnold Engineering Development Center ARO, Inc., Operating Contractor Arnold Air Force Station, Tennessee	2a REPORT SECURITY CLASSIFICATION UNCLASSIFIED 2b GROUP N/A

3 REPORT TITLE

INVESTIGATION OF THE EFFECT OF FLARE AND RAMP ANGLE ON THE UPSTREAM INFLUENCE OF LAMINAR AND TRANSITIONAL REATTACHING FLOWS FROM MACH 3 TO 7

4 DESCRIPTIVE NOTES *(Type of report and inclusive dates)*

N/A

5 AUTHOR(S) *(Last name, first name, initial)*

Gray, J. Don, ARO, Inc.

6 REPORT DATE January 1967	7a TOTAL NO OF PAGES 68	7b. NO OF REFS 26

8a CONTRACT OR GRANT NO. AF40(600)-1200 b. PROJECT NO. 8219 c Program Element 62405364 d Task 821902	9a. ORIGINATOR'S REPORT NUMBER(S) AEDC-TR-66-190 9b OTHER REPORT NO(S) *(Any other numbers that may be assigned this report)* N/A

10 AVAILABILITY/LIMITATION NOTICES

Distribution of this document is unlimited.

11 SUPPLEMENTARY NOTES Available in DDC	12. SPONSORING MILITARY ACTIVITY Arnold Engineering Development Center Air Force Systems Command Arnold Air Force Station, Tennessee

13 ABSTRACT

An experimental investigation of laminar- and transitional-flow separation induced by flares and ramps of different angles was conducted at Mach numbers 3, 5, and 7 over a broad unit Reynolds number range. Surface pressure distributions, schlieren and shadowgraph pictures, and the oil film technique were used to determine the effect of transition during flow reattachment on the scale of laminar separation. It is concluded that because transition is always triggered prematurely by the reattachment pressure gradient, small flow deflections ($\theta \leq 10$ deg) are required when investigating laminar reattaching flows at similar test conditions. The scale of separation increased with unit Reynolds number increase, and the pressure distribution upstream of the flare was characterized by the absence of any lengthy plateau whenever the flow was laminar through the reattachment zone. Nose blunting reduced the extent of such separations.

DD FORM 1 JAN 64 1473

Security Classification

14. KEY WORDS	LINK A ROLE	LINK A WT	LINK B ROLE	LINK B WT	LINK C ROLE	LINK C WT
flares						
ramps						
transitional flow						
laminar separation						
surface pressures						

INSTRUCTIONS

1. ORIGINATING ACTIVITY: Enter the name and address of the contractor, subcontractor, grantee, Department of Defense activity or other organization *(corporate author)* issuing the report.

2a. REPORT SECURITY CLASSIFICATION: Enter the overall security classification of the report. Indicate whether "Restricted Data" is included. Marking is to be in accordance with appropriate security regulations.

2b. GROUP: Automatic downgrading is specified in DoD Directive 5200.10 and Armed Forces Industrial Manual. Enter the group number. Also, when applicable, show that optional markings have been used for Group 3 and Group 4 as authorized.

3. REPORT TITLE: Enter the complete report title in all capital letters. Titles in all cases should be unclassified. If a meaningful title cannot be selected without classification, show title classification in all capitals in parenthesis immediately following the title.

4. DESCRIPTIVE NOTES: If appropriate, enter the type of report, e.g., interim, progress, summary, annual, or final. Give the inclusive dates when a specific reporting period is covered.

5. AUTHOR(S): Enter the name(s) of author(s) as shown on or in the report. Enter last name, first name, middle initial. If military, show rank and branch of service. The name of the principal author is an absolute minimum requirement.

6. REPORT DATE: Enter the date of the report as day, month, year, or month, year. If more than one date appears on the report, use date of publication.

7a. TOTAL NUMBER OF PAGES: The total page count should follow normal pagination procedures, i.e., enter the number of pages containing information.

7b. NUMBER OF REFERENCES: Enter the total number of references cited in the report.

8a. CONTRACT OR GRANT NUMBER: If appropriate, enter the applicable number of the contract or grant under which the report was written.

8b, 8c, & 8d. PROJECT NUMBER: Enter the appropriate military department identification, such as project number, subproject number, system numbers, task number, etc.

9a. ORIGINATOR'S REPORT NUMBER(S): Enter the official report number by which the document will be identified and controlled by the originating activity. This number must be unique to this report.

9b. OTHER REPORT NUMBER(S): If the report has been assigned any other report numbers *(either by the originator or by the sponsor)*, also enter this number(s).

10. AVAILABILITY/LIMITATION NOTICES: Enter any limitations on further dissemination of the report, other than those imposed by security classification, using standard statements such as:

(1) "Qualified requesters may obtain copies of this report from DDC."

(2) "Foreign announcement and dissemination of this report by DDC is not authorized."

(3) "U. S. Government agencies may obtain copies of this report directly from DDC. Other qualified DDC users shall request through _____."

(4) "U. S. military agencies may obtain copies of this report directly from DDC. Other qualified users shall request through _____."

(5) "All distribution of this report is controlled. Qualified DDC users shall request through _____."

If the report has been furnished to the Office of Technical Services, Department of Commerce, for sale to the public, indicate this fact and enter the price, if known.

11. SUPPLEMENTARY NOTES: Use for additional explanatory notes.

12. SPONSORING MILITARY ACTIVITY: Enter the name of the departmental project office or laboratory sponsoring *(paying for)* the research and development. Include address.

13. ABSTRACT: Enter an abstract giving a brief and factual summary of the document indicative of the report, even though it may also appear elsewhere in the body of the technical report. If additional space is required, a continuation sheet shall be attached.

It is highly desirable that the abstract of classified reports be unclassified. Each paragraph of the abstract shall end with an indication of the military security classification of the information in the paragraph, represented as *(TS)*, *(S)*, *(C)*, or *(U)*.

There is no limitation on the length of the abstract. However, the suggested length is from 150 to 225 words.

14. KEY WORDS: Key words are technically meaningful terms or short phrases that characterize a report and may be used as index entries for cataloging the report. Key words must be selected so that no security classification is required. Identifiers, such as equipment model designation, trade name, military project code name, geographic location, may be used as key words but will be followed by an indication of technical context. The assignment of links, rules, and weights is optional.